Appendix L

Regional Earthquake Reports
PG&E Geosciences Department

L-1: Deer Canyon Earthquakes of October 18, 2003

L-2: San Simeon Earthquake of December 22, 2003

L-3: Mw 6.0 Parkfield Earthquake of September 28. 2004

Appendix L-1

Deer Canyon Earthquakes of October 18, 2003

Diablo Canyon Power Plant
Deer Canyon earthquakes of October 18, 2003

Two small (M_L 3.4) earthquakes occurred on October 18, 2003 at 12:27 and 12:38 AM PDT (07:27 and 07:38 GMT). The events are located approximately 4 km east of Diablo Canyon Power Plant (DCPP), in the region northwest of Deer Canyon. Both earthquakes were felt in the Unit 1 control room; the second event triggered strong motion instruments at the plant site. The earthquakes are part of a sequence of 14 small earthquakes that occurred between October 12 and October 24, 2003. The following is a report describing the earthquake sequence and strong motion recordings from the plant.

Earthquake Sequence

The Deer Canyon earthquakes were recorded by the PG&E Central Coast Seismic Network (CCSN). The CCSN has operated since 1987 as part of the PG&E Long Term Seismic Program. The CCSN data are augmented by recordings from the U.S. Geological Survey's (USGS) Northern California Seismic Network (NCSN). The CCSN consists of 20 seismographic stations, including five dual-gain 3-component stations (large triangles in inset to Figure 1). The addition of the CCSN, including the three-component stations greatly improves the accuracy of the earthquake locations in the region around DCPP.

The earthquakes are located using the velocity model and station corrections from McLaren and Savage (2000). Duration magnitudes (M_D) also are estimated from the CCSN data. The earthquake location parameters for the 14 events in the sequence are listed in Table 1. Events 1, 4, 5, 11, 12, and 13 (Table 1) were recorded by both the CCSN and NCSN; the combined data from the two networks were used in the locations for these six events.

The Deer Canyon earthquake locations generally are well constrained. Except for event 6, all of the events have small (<1 km) horizontal and vertical depth errors and all have low (<.20 sec) Root Mean Square (RMS) residuals. Except for event 14, all have at least 1 S-wave reading from a station that is at about 1 focal depth distance from the epicenter, providing good depth control.

Figure 1 shows the Deer Canyon sequence with previous earthquakes for the period 1987 to the present. The previous earthquakes were located using the same velocity model and station corrections as the current sequence.

The two magnitude 3 earthquakes of October 18 have similar characteristics. The USGS local magnitude (M_L) for both events is 3.4 (http://usgs.wr.gov); the duration magnitudes (M_D) from the CCSN for the two events are 3.4 and 3.3 for the 12:27 AM and 12:38 AM events, respectively. The earthquake depths also are similar: 6.5 and 6.7 km. (The USGS website reports depths of 2.3 and 2.5 km, respectively, however, due to the better coverage of the combined network and S-wave data, our depths are more accurate.)

Lastly, the focal mechanisms of the two events (events 4 and 5 of Figure 2) both show normal oblique slip.

The Deer Canyon sequence consists of 14 earthquakes with magnitudes ranging from 0.4 to 3.4. Three small earthquakes preceded the October 18 magnitude 3 mainshocks: two on October 12 with magnitudes of 2.3 and 0.5, and one magnitude 1.7 event on October 17. Nine aftershocks have occurred up through October 24 with magnitudes less than M2.6. The first preshock (event 1 of Table 1) occurred in the same depth range (6.5 km) as the two magnitude 3 earthquakes. The second two preshocks and nearly all of the aftershocks are located in a narrow depth range at about 3.7 km; the exception is event 11 that was located at a depth of 8.9 km. This deeper event was located away from the other aftershocks, about 7 km NW of the mainshocks (Figure 1).

The Deer Canyon earthquakes occurred within the San Luis/Pismo structural block. The San Luis/Pismo structural block is one of three distinct uplifting structural blocks of the Los Osos domain (Lettis et al, 2001). The block is bounded on the west by the Hosgri fault zone and on the northeast and southwest by west-northwest-trending, high-angle reverse Quaternary faults (Los Osos and Southwest boundary fault zones of Figure 1); crustal shortening is accommodated primarily by reverse faulting along the northwest trending block margins (Lettis, et al. 2001).

The San Luis/Pismo block is highly fractured. Figure 1 shows the Deer Canyon sequence and the previous earthquakes. The previous seismicity shows scattered activity across the San Luis/Pismo block; the Deer Canyon earthquakes locate within this region of previous activity.

Cross section AA' perpendicular to the long axis of the block (Figure 1) shows that the previous seismicity is approximately uniformly distributed in depth. The depth range of the main Deer Canyon sequence, from 3.4 to 6.7 km, is consistent with the depth range of the previous seismicity.

Earthquakes occurring within the block generally have had a variety of focal mechanisms (Figure 2). The normal oblique mechanisms for the magnitude 3 events on October 18 and the reverse mechanisms of aftershocks 11 and 13 are consistent with the mechanisms of past earthquakes in this region.

Strong ground motion

Both earthquakes were felt in the Unit 1 control room; the operators reported that the second event was the stronger. The first event did not trigger the seismic instruments. The second event did not trigger the Basic Seismic System analog recorder (Kinemetrics SMA) in the control room, however the Kinemetrics digital recorders (SSA) at the Unit 1 containment base, top of containment, the auxiliary building, and the free-field pit location (near the fitness trailer) did trigger on the second event. According to David Castleman of Kinemetrics, Inc., the SMA system worked properly; however, the system did not trigger because the containment base ground motions contained significant energy

outside the 1.0 to 10.0 Hz bandwidth of the SMA trigger. The Supplemental System was inoperable at the time of the earthquakes; however, three temporary accelerometers (TerraTech GSR-18), located in the Auxiliary and the Turbine buildings, recorded the second event. The peak accelerations are listed in Table 2.

The earthquake force monitor (EFM) located in the control room measured 0.02g on the vertical component. The EFM measurement is from the sensor at the Unit 1 Containment base and does not have the DC offset removed. If the DC offset is removed, the peak acceleration on the vertical component is 0.011g.

The ground motions from the free-field and containment base were corrected by removing the DC offset, filtering the long period noise, and removing the baseline drift. First, the DC offset was removed using the average of the first 50 samples from the pre-event part of the accelerogram. Next, the accelerograms were high-pass filtered using a 4-pole Butterworth filter with a corner-frequency at 1 Hz. This corner-frequency was selected by evaluating the Fourier spectrum of the unfiltered accelerations which indicated noise at periods greater than 1 second. Finally, the baseline drift was removed using a high-order polynomial (without the constant and linear terms) fit to the displacement waveform. The corrected acceleration, velocity, and displacement time seismograms for the three components of motion at the free-field stations are shown in Figures 3a, 3b, and 3c. Similar plots of the acceleration, velocity, and displacement seismograms for the Unit 1 containment base are shown in Figures 4a, 4b, and, 4c. These seismograms show that the shaking at the DCPP site had a duration of strong shaking of 3 seconds. The containment base recordings appear to still have long period noise at a frequency of about 1 Hz that was not completely removed by the filtering (see displacement seismograms in Figures 4a, 4b, and 4c). Additional filtering could remove this noise, but it would also begin to affect the part of the ground motion that is not noise (e.g. at the S-wave arrival). This noise does not affect the peak values.

Table 3 lists the peak accelerations, peak velocities, and peak displacements of the free-field and Unit 1 containment base ground motions after the filtering and baseline corrections are applied. The peak accelerations range between about 1 to 2% g with the largest peak acceleration on the vertical component.

The response spectra were computed for the free-field and Unit 1 containment base recordings. The 5% damped spectra for the free-field and Unit 1 containment base recordings are shown in Figure 5 and 6, respectively. The response spectra for this earthquake show very high frequency content that is typical for an earthquake of this magnitude. For the free-field, the horizontal spectra peak at about 12 Hz and the vertical spectrum peaks at about 20 Hz. For the Unit 1 containment base, the peaks are shifted to slightly smaller frequencies. This shift to lower frequencies is an expected effect of the large foundation. The ratio of the average horizontal response spectrum from the containemt base to the free-field station is shown in Figure 7. This response spectral ratio shows the reduction in high frequency content on the containment base compared to the free-field recording.

The magnitude of the earthquake is too small to reliably use standard empirical attenuation relations to evaluate the strength of the ground motion. As an alternative to empirical attenuation relations, the ground motion can be evaluated using the stochastic point source model (Boore, 2000). The stochastic model is used to estimate the ground motion expected for a (moment) magnitude 3.4 earthquake at a hypocentral distance of 7.8 km for typical rock site conditions in California. The response spectrum computed for a stress-drop of 120 bars and a kappa of 0.042 seconds is compared to the average horizontal spectrum from the free-field recording in Figure 8. This comparison shows that the frequency content of the free-field ground motion is consistent with the expected frequency content for a magnitude 3.4 earthquake with a kappa value that is typical of California rock sites. The level of shaking is consistent with a stress-drop of 120 bars. A stress-drop of 120 bars is higher than average for California earthquakes, but it is within the range of observed stress-drops for small magnitude events. The underestimation of the ground motion at frequencies less than 3 Hz may indicate that the moment magnitude is greater than 3.4 (e.g. the M_L may be underestimating the moment magnitude for this event). If the moment magnitude is 3.5, then the fit to the lower frequencies is improved and the stress-drop is reduced to 85 bars which is close to the average stress-drop for small earthquakes in California.

Conclusions

The occurrence, location, and magnitude of the October 18, 2003 Deer Canyon earthquakes is not a surprise as the sequence of earthquakes is consistent with our understanding of the tectonic framework in the region around DCPP. The events occurred in the San Luis/Pismo block, which is a region of previous seismicity. Additional small earthquakes are expected to occur in this block.

The ground motions from the second event (12:38 AM) are typical for ground motions from a magnitude 3.4 earthquake at a distance of 7.8 km on a rock site condition.

References

Boore, D. M (2000). SMSIM – Fortran programs for simulating ground motions from earthquakes: version 2.0 – a revision of OFR 96-80-A, U.S. Geological Survey OFR 00-509.

Lettis, W. R., Hanson, K. L., Unruh, J. R., McLaren, M. K., and Savage, W. U. (2001) Quaternary tectonic setting of south-central coastal California, in *Evolution of Sedimentary basins/onshore oil and gas investigations- Santa Maria Province*, M. A. Keller (Editor), *U. S. Geol. Survey Bull*. (in press)

McLaren, M. K. and Savage, W. U. (2000). Seismicity of South-Central Coastal California: October 1987 through January 1997, *Bull Seism. Soc. Am.* **91**, no. 6, pp. 1629-1658.

Pacific Gas and Electric Company (1988), Final report of the Diablo Canyon long term seismic program, U.S. Nuclear Regulatory commission docket Nos. 50-75 and 50-23.

Report prepared by Ms. Marcia McLaren and Dr. Norman Abrahamson of the PG&E Geosciences Dept.

Date: November 5, 2003

Table 1: Earthquake location parameters for the Deer Canyon sequence, 10/12/03 to 10/24/03.
Felt events are highlighted in gray.

No.	Date	Time (UTC)	Lat	Lon	Depth	No. P- & S-wave readings	Gap btwn stas. (deg)	Dist. to nearest station (km)	RMS (sec)	*M_D	No. S-wave readings	Horiz. Error (km)	Vert. Error (km)	No. P-wave first motions
1	10/12/2003	13:32 28.54	35 11.97	-120 48.83	6.6	52	145	3	0.13	2.3	2	0.41	0.39	43
2	10/12/2003	16:57 37.60	35 12.28	-120 47.59	3.8	6	137	3	0.07	0.5	1	0.66	0.33	5
3	10/17/2003	13:19 14.33	35 12.49	-120 47.88	3.6	34	123	3	0.14	1.7	4	0.37	0.17	30
4	10/18/2003	07:27 18.37	35 12.23	-120 48.53	6.5	57	125	3	0.12	3.4	2	0.23	0.39	101
5	10/18/2003	07:38 59.14	35 12.15	-120 48.52	6.7	60	127	3	0.12	3.3	2	0.25	0.35	112
6	10/18/2003	07:40 49.52	35 12.10	-120 47.81	3.7	6	149	4	0.05	0.4	1	3.09	1.79	5
7	10/18/2003	07:41 43:44	35 12.18	-120 47.92	3.7	9	147	4	0.09	1.1	1	0.85	0.44	8
8	10/18/2003	07:55 18.96	35 12.13	-120 47.88	3.7	16	132	4	0.12	1.3	3	0.52	0.21	11
9	10/20/2003	10:38 21.93	35 12.24	-120 47.97	3.6	9	146	4	0.07	1.1	1	0.61	0.31	7
10	10/20/2003	18:22 37.72	35 12.35	-120 48.05	3.8	9	142	3	0.07	0.9	1	0.67	0.33	8
11	10/20/2003	19:28 31.85	35 15.05	-120 44.37	8.9	46	50	4	0.10	1.5	3	0.43	0.61	15
12	10/21/2003	08:35 40.18	35 12.43	-120 48.00	3.6	24	125	3	0.11	1.2	2	0.54	0.25	12
13	10/21/2003	13:43 36.44	35 12.65	-120 48.20	3.7	37	119	3	0.12	2.6	3	0.36	0.17	41
14	10/24/2003	23:30 52.84	35 12.06	-120 47.73	3.4	6	147	4	0.07	0.7	0	0.52	0.33	6

***M_D** = duration magnitude

Table 2. Digital peak acceleration recordings from the Basic and temporary Supplemental systems (DC offset removed, prior to filtering and baseline correction)

Instrument type	**Instrument location**	**Peak Accelerations (g)**		
		Channel 1 (Horiz 1)	**Channel 2 (Vertical)**	**Channel 3 (Horiz 2)**
Kinemetrics SSA	Free field pit (near admin bldg)	-0.020	-0.022	0.011
Kinemetrics SSA	Unit 1 Containment base, 89’ elev.	-0.008	-0.011	-0.009
Kinemetrics SSA	Unit 1 top of Containment	-0.032	0.14	-0.024
Kinemetrics SSA	Auxiliary Bldg, 64 ‘ elev.	0.005	0.010	0.006
Terratech GSR-18	Auxiliary Bldg, 64’ elev.	0.009	0.021	-0.011
Terratech GSR-18	Turbine Bldg Unit 1, 85’ elev.	0.013	0.024	0.009
Terratech GSR-18	Turbine Bldg Unit 2, 85’ elev.	0.010	0.024	-0.014
Terratech GSR-18	500 KV switchyard control room basement	0.025	0.013	0.014

Table 3. Peak ground motions values from the Basic Seismic System digital recorders (after filtering and baseline correction)

Instrument type	**Instrument location**	**Component**	**Peak Acceleration (g)**	**Peak Velocity (cm/s)**	**Peak Displacement (cm)**
Kinemetrics SSA	Free field pit (near fitness trailer)	Horizontal 1 (Channel 1)	0.020	0.32	0.0100
		Vertical (Channel 2)	0.022	0.19	0.0042
		Horizontal 2 (Channel 3)	0.011	0.19	0.0068
Kinemetrics SSA	Unit 1 Containment base, 89' elev.	Horizontal 1 (Channel 1)	0.008	0.16	0.0077
		Vertical (Channel 2)	0.012	0.16	0.0060
		Horizontal 2 (Channel 3)	0.009	0.22	0.0094

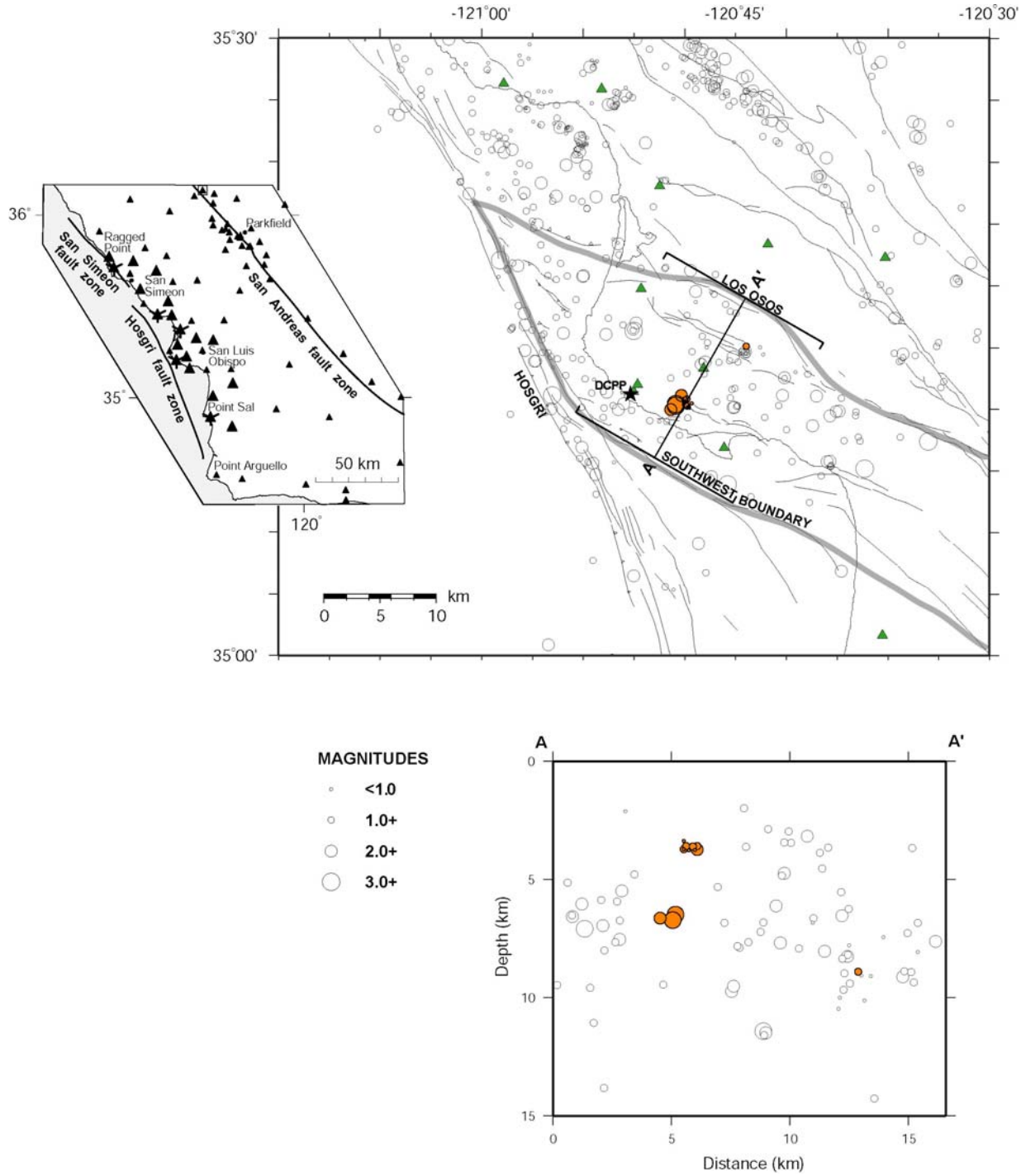

Figure 1. Map and seismic cross section showing the Deer Canyon sequence (orange circles) from October 12 through October 24, 2003 with previous earthquakes (grayed circles) from October 1987 to October 11, 2003. The data were recorded by the PG&E Central Coast Seismic network (large triangles on top figure inset; triangles with tick marks are 3-component stations) and the Northern California Seismic network (small triangles on top figure inset). Seismic stations also are shown on larger map(green triangles). Location of seismic cross section AA' is shown on map with 8-km-wide bars to mark events projected on to the cross section in bottom figure. Quaternary faults are from PG&E (1988); selected faults are labeled. The thick gray line is the boundary of the San Luis/Pismo structural block (Lettis and others, 2001).

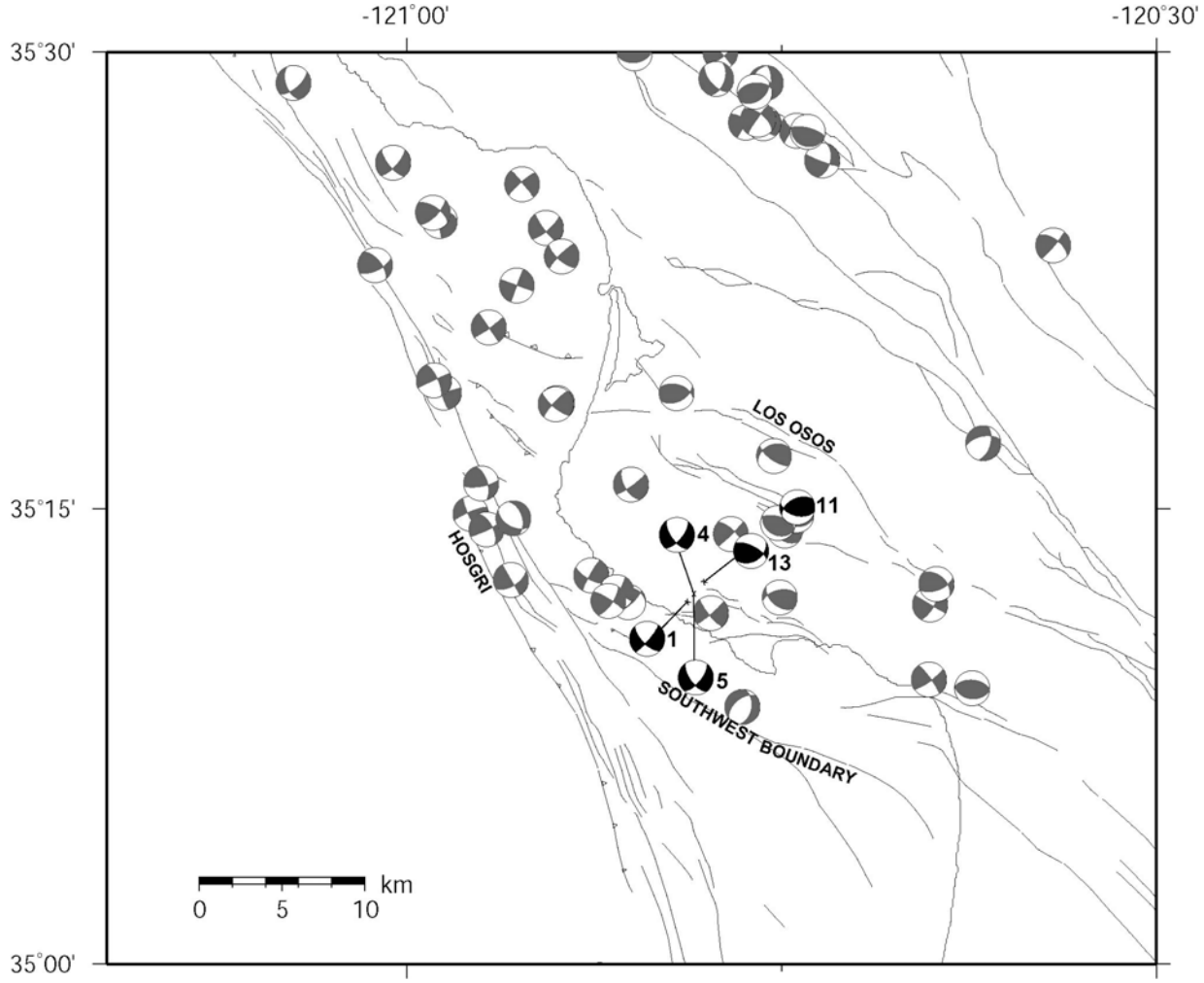

Figure 2. Lower hemisphere P-wave focal mechanisms. Grayed mechanisms are from McLaren and Savage (2000) for the time period October 1997 through January1997. Darker mechanisms are from the Deer Canyon sequence and are numbered according to Table 1. See Figure 1 for fault description.

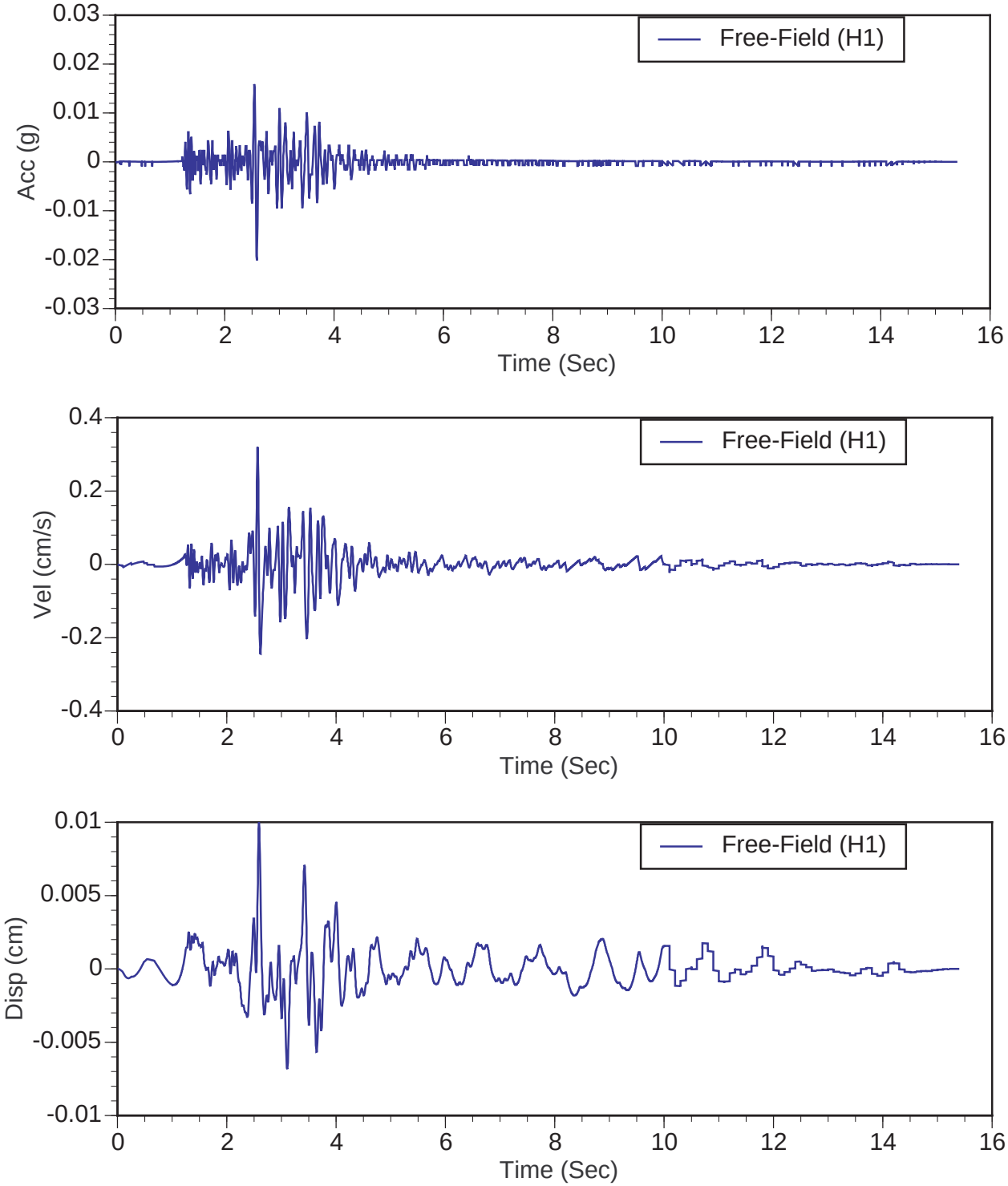

Figure 3a. Acceleration, velocity, and displacement for the horizontal 1 component (channel 1) of the free-field recording after filtering and baseline correction.

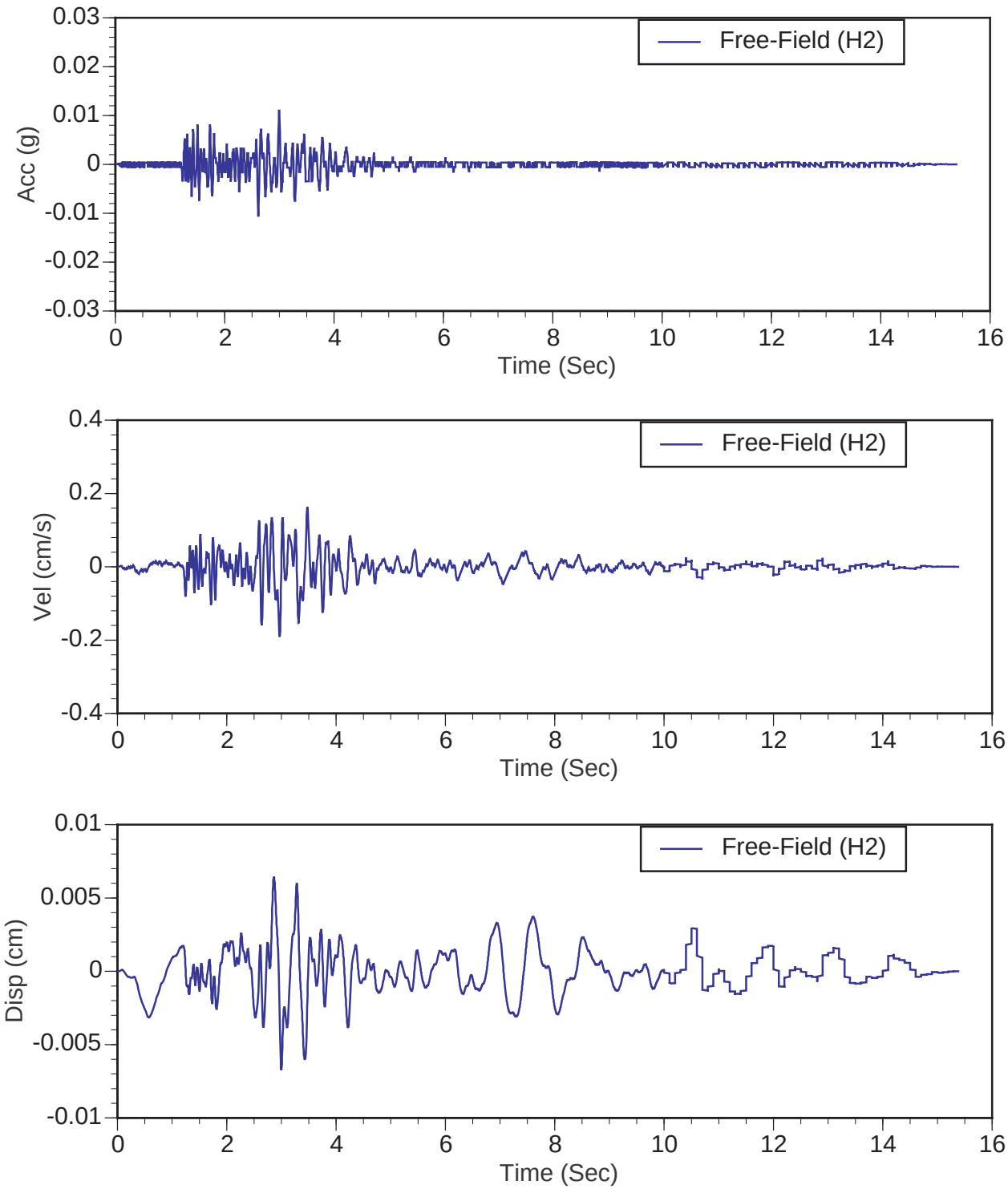

Figure 3b. Acceleration, velocity, and displacement for the horizontal 2 component (channel 3) of the free-field recording after filtering and baseline correction.

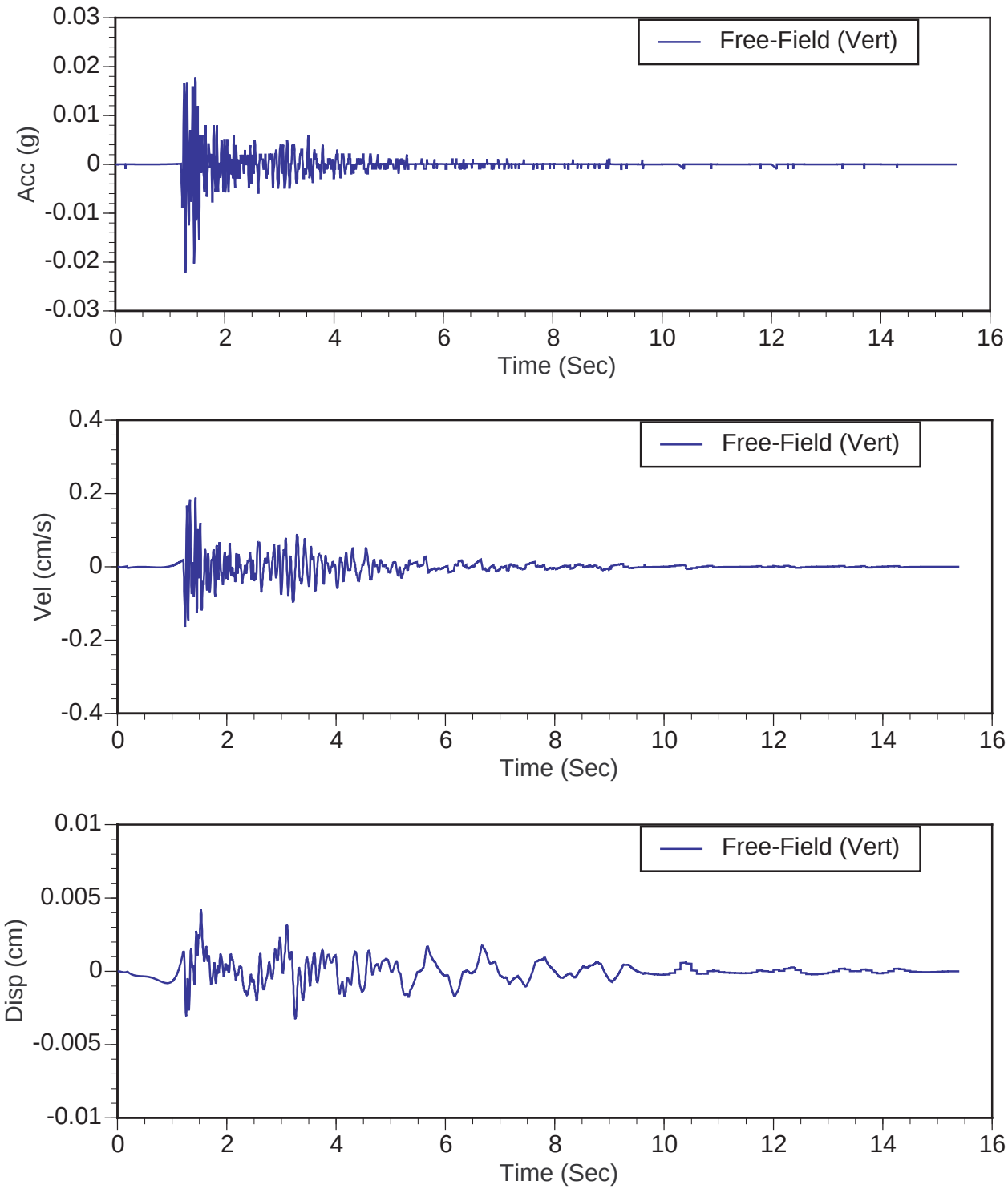

Figure 3c. Acceleration, velocity, and displacement for the vertical component (channel 2) of the free-field recording after filtering and baseline correction.

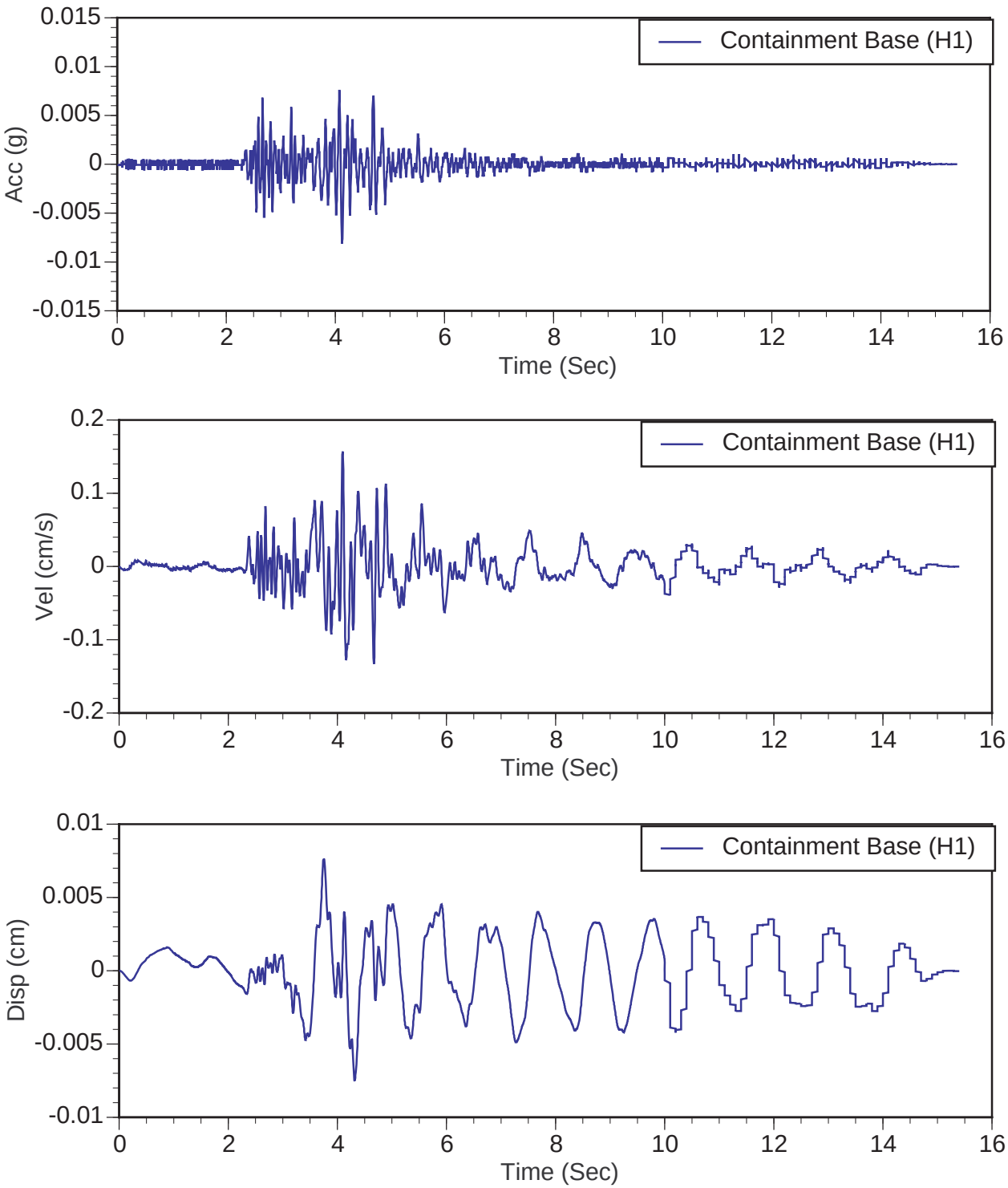

Figure 4a. Acceleration, velocity, and displacement for the horizontal 1 component (channel 1) of the unit 1 containment base recording after filtering and baseline correction. There is still some noise in the displacements at a frequency of about 1 Hz.

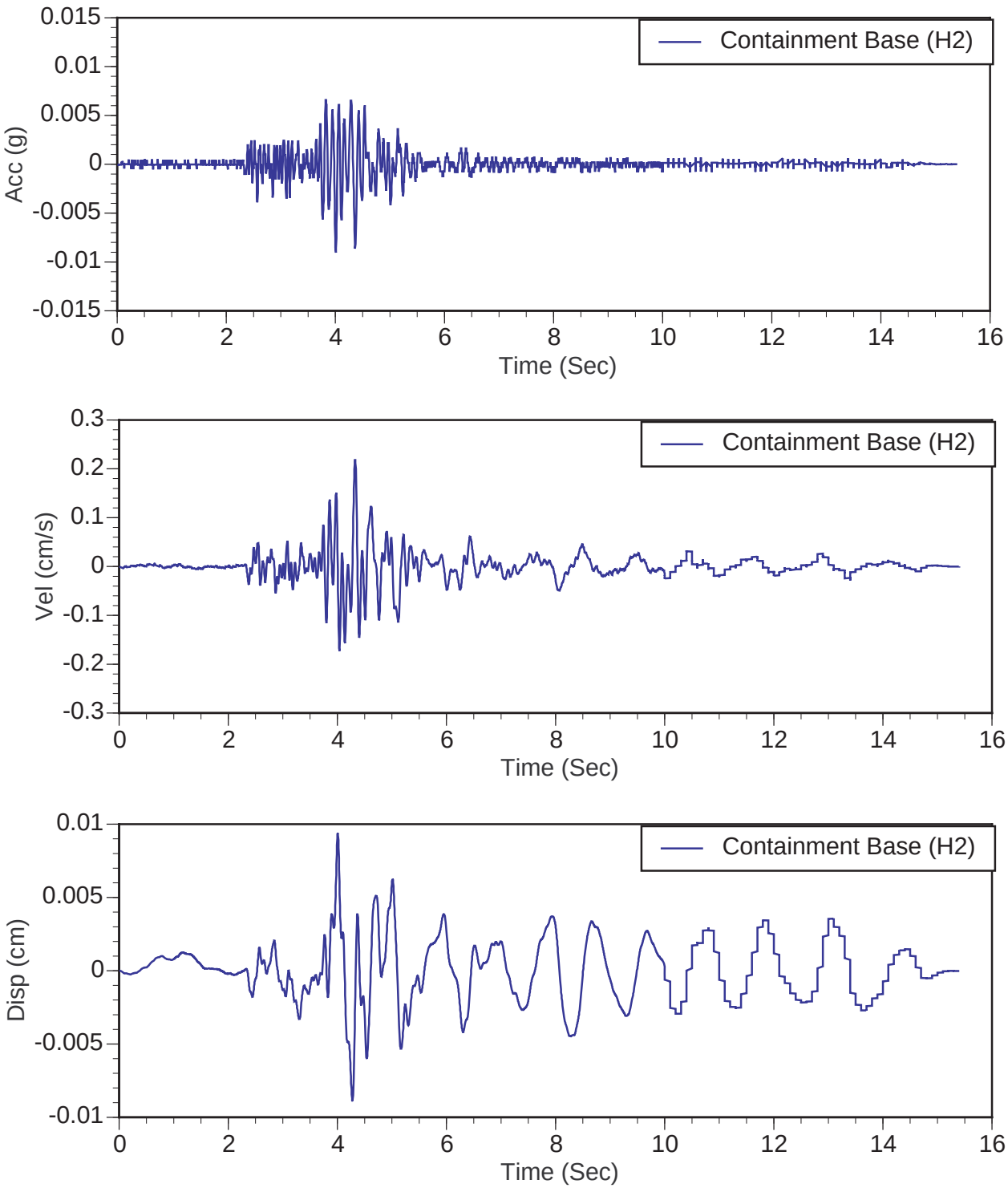

Figure 4b. Acceleration, velocity, and displacement for the horizontal 2 component (channel 3) of the unit 1 containment base recording after filtering and baseline correction. There is still some noise in the displacements at a frequency of about 1 Hz.

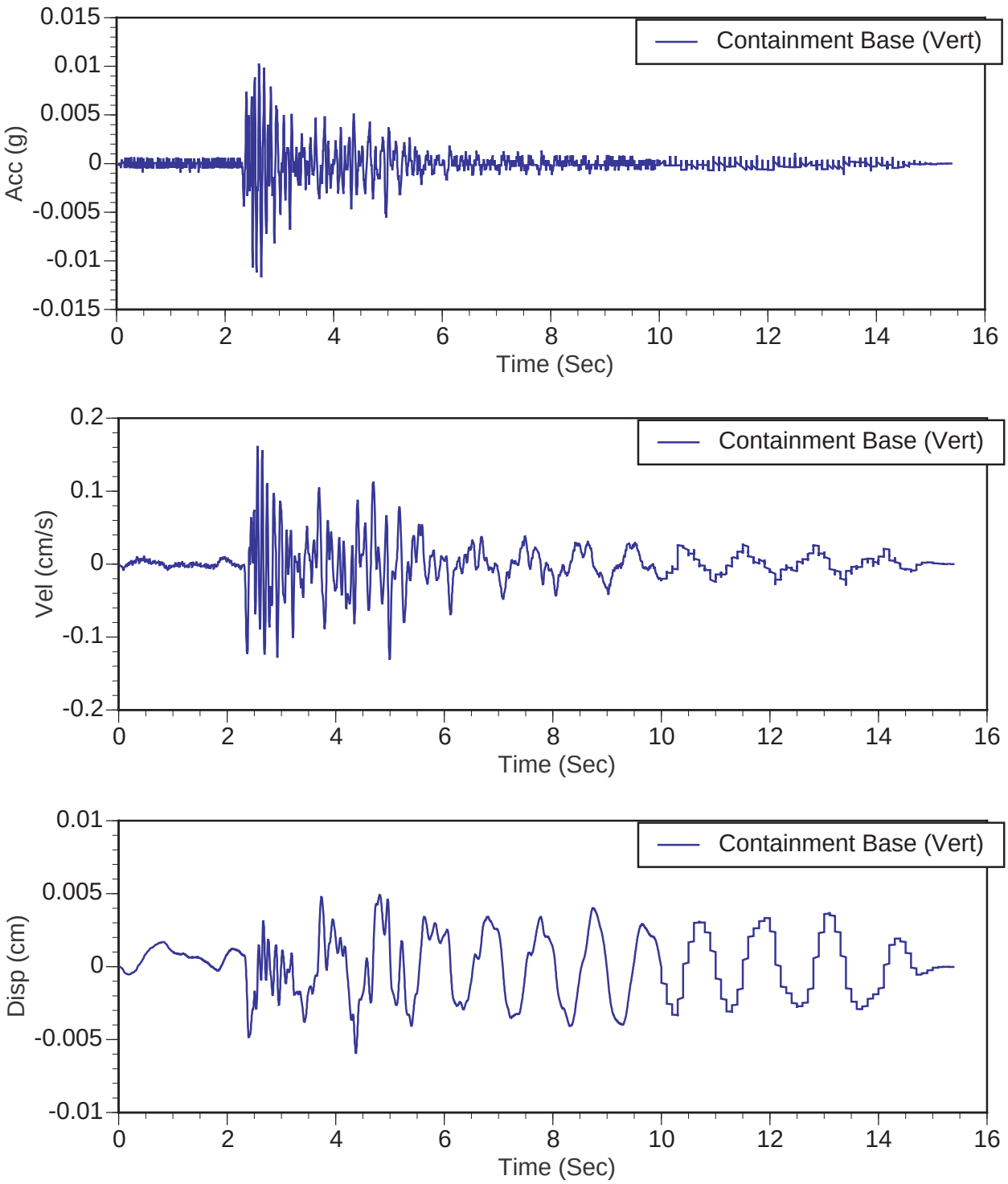

Figure 4c. Acceleration, velocity, and displacement for the vertical component (channel 2) of the unit 1 containment base recording after filtering and baseline correction. There is still some noise in the displacements at a frequency of about 1 Hz.

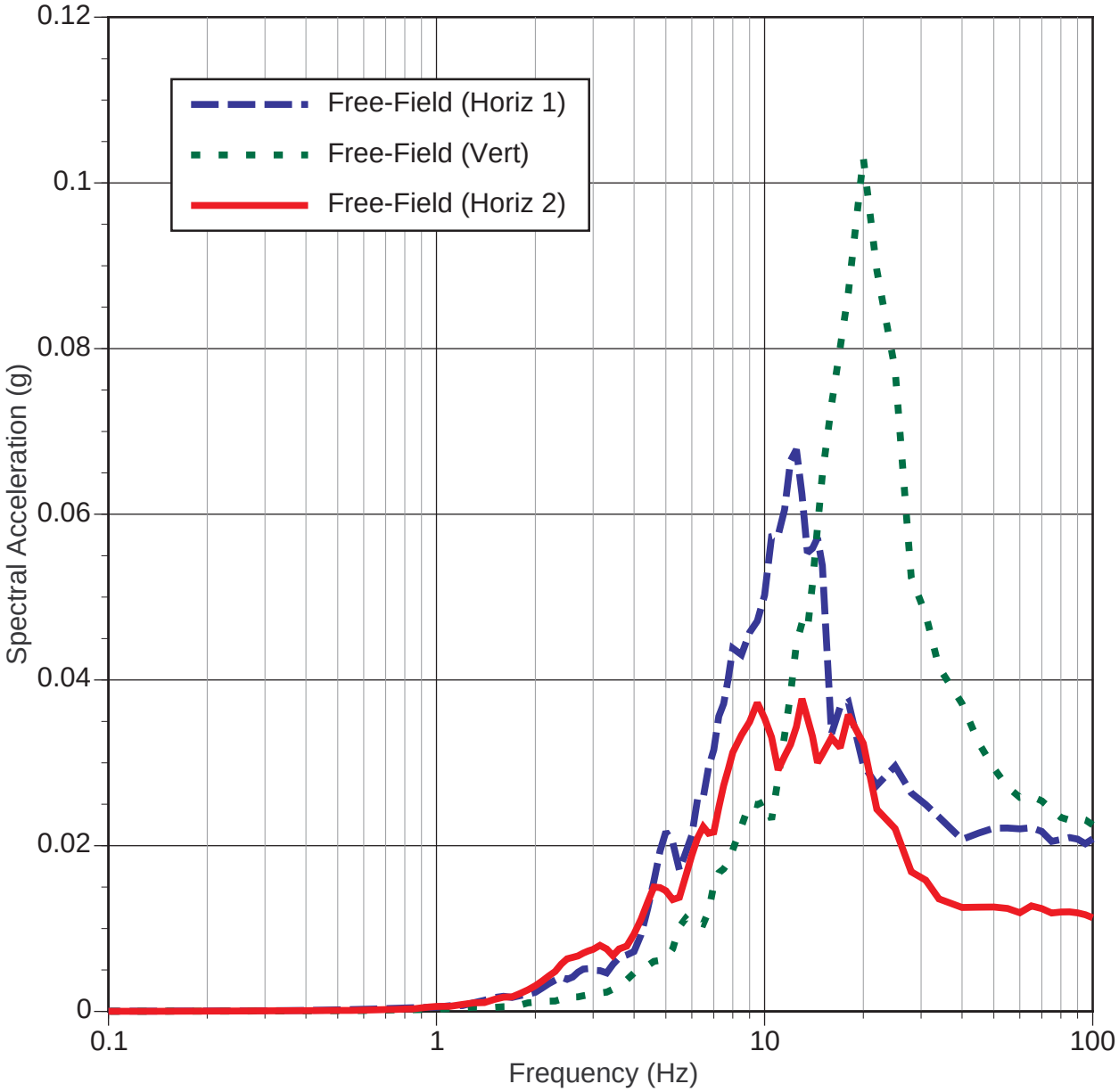

Figure 5. Response spectra at 5% damping for the free-field ground motion.

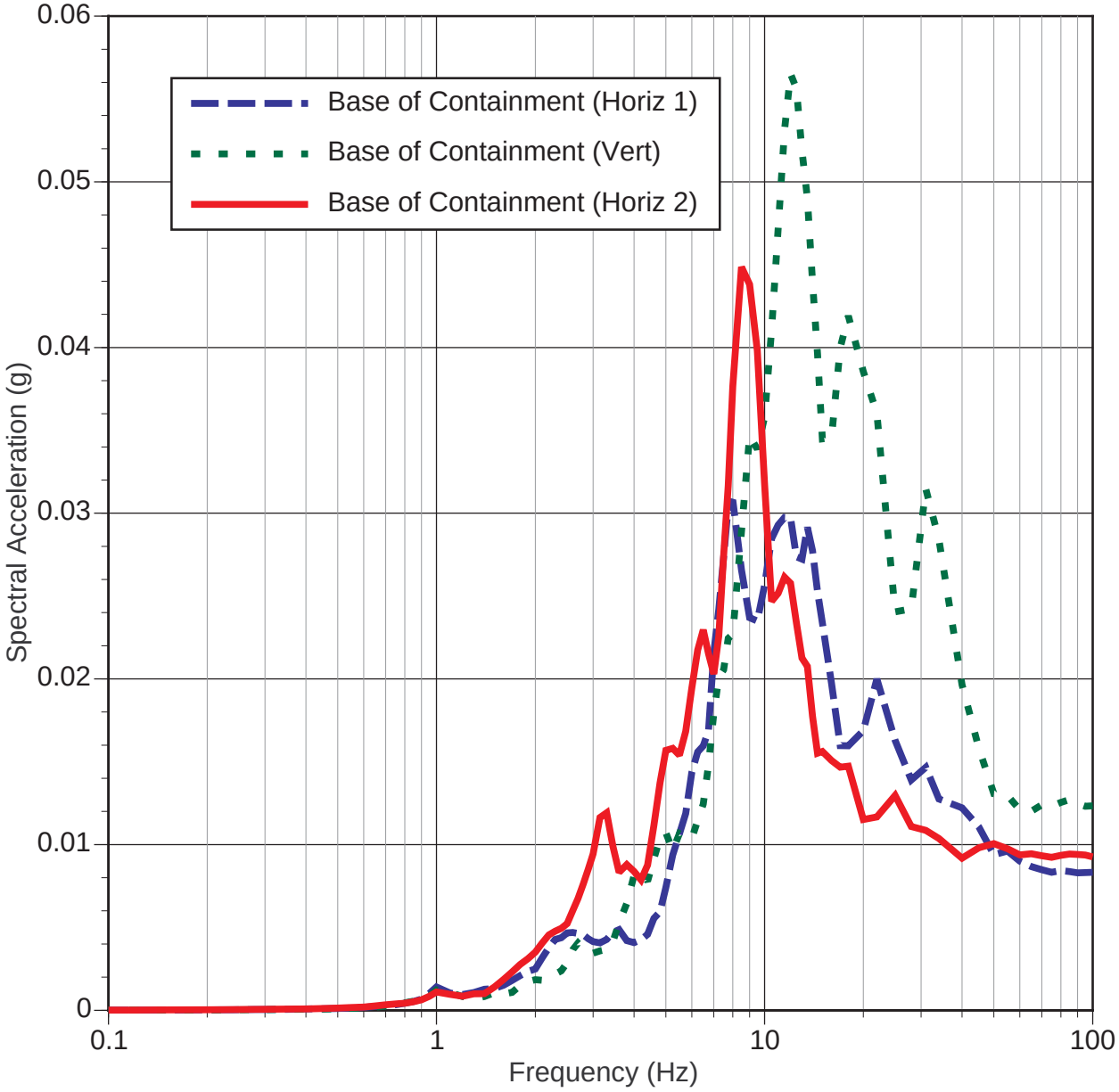

Figure 6. Response spectra at 5% damping for the unit 1 containment base ground motion.

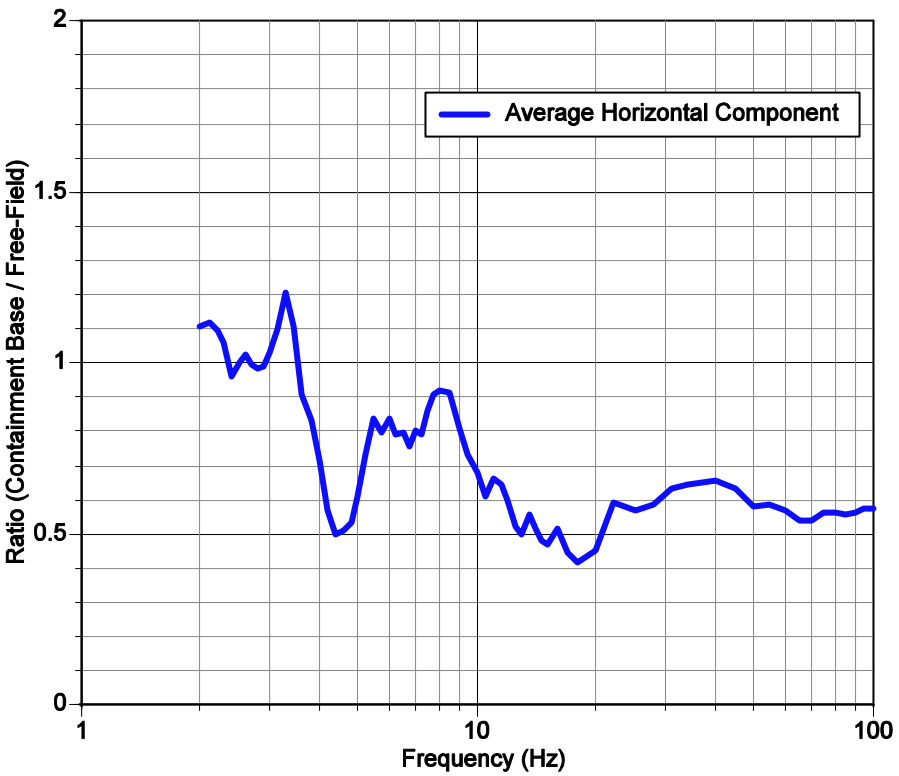

Figure 7. Response spectral ratio (5% damping) of the average horizontal component at at containment base of unit 1 to the free-field. The spectral ratio is only plotted for frequencies greater than 2 Hz because there is noise in the containment base recordings at frequencies less than 2 Hz.

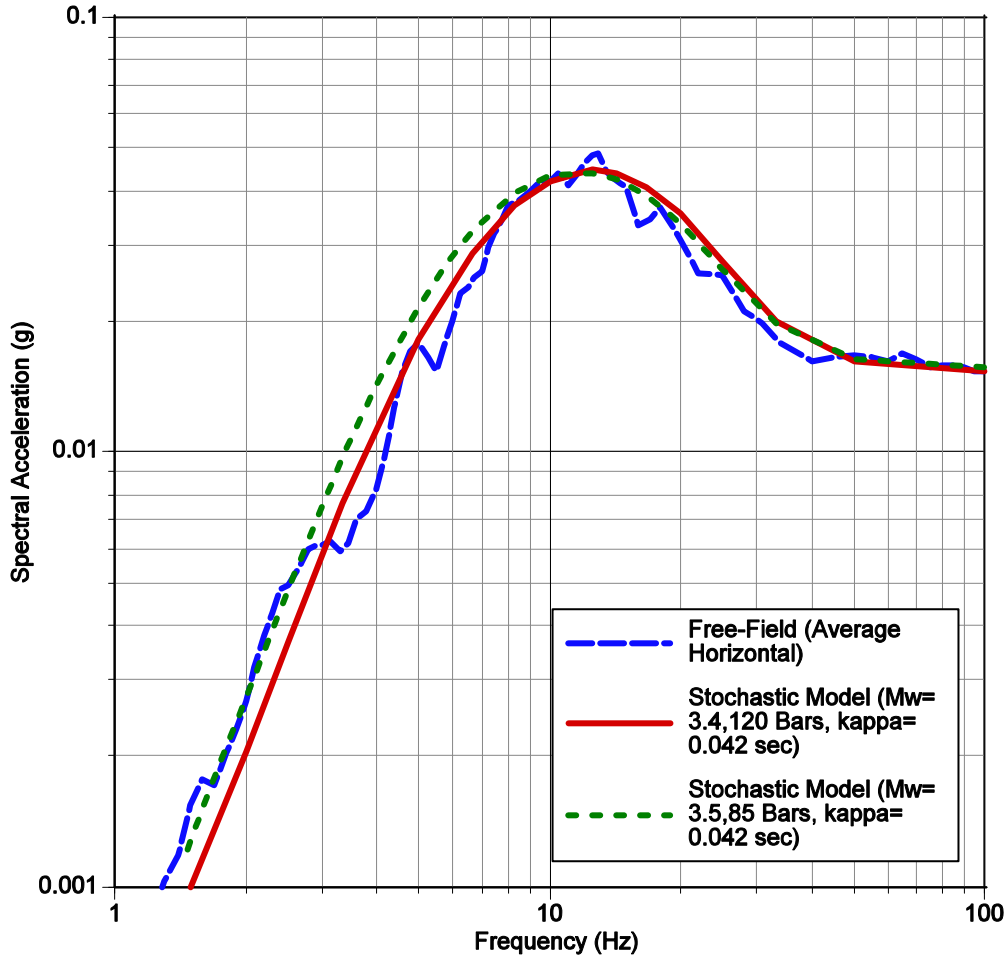

Figure 8. Comparison of the average horizontal response spectrum at 5% damping for the free-field recording with the expected California rock site spectrum from a moment magnitude 3.4 earthquake at a distance of 7.8 km with a stress-drop of 120 bars and kappa of 0.042 sec based on the stochastic point source model (red curve). The green curve shows the spectrum if the moment magnitude is 3.5 with a stress-drop of 85 bars.

Appendix L-2

San Simeon Earthquake of December 22, 2003

January 5, 2004

PG&E Letter No. DCL-03-184

U.S. Nuclear Regulatory Commission
ATTN: Document Control Desk
Washington, DC 20555-0001

Docket No. 50-275, OL-DPR-80
Docket No. 50-323, OL-DPR-82
Diablo Canyon Units 1 and 2
Special Report 03-04: San Simeon Earthquake of December 22, 2003

Dear Commissioners and Staff:

On December 22, 2003, at 1116 PST, with Unit 1 and Unit 2 operating at 100 percent power, a 6.5 magnitude earthquake occurred 11 km northeast of San Simeon, California. Ground motion was felt and recognized as an earthquake by the control room operators. The earthquake force monitor recorded greater than 0.01g for the seismic event. Operations personnel declared an Unusual Event at 1122 PST. (Reference NRC Event Notification Number 40408.) On December 23, 2003, at 1212 PST, the Unusual Event was terminated upon confirmation that no damage to the plant occurred.

This special report is submitted pursuant to Equipment Control Guideline (ECG) 51.1, "Seismic Instrumentation." This ECG requires the following actions for a seismic event: for seismic monitoring instruments actuated during a seismic event, "data shall be retrieved from actuated instruments and analyzed to determine the magnitude of the vibratory ground motion. A special report shall be prepared and submitted to the Commission … describing the magnitude, frequency spectrum, and resultant effect upon facility features important to safety."

Enclosure 1 describes the ground motion analysis including the magnitude and frequency spectrum of this event. Enclosure 2 provides an analysis of the resultant effect upon facility features important to safety.

As this event relates to the Diablo Canyon Power Plant, there was no adverse effect to public health and safety, or upon facility features important to safety.

If you have any questions, please contact me at 805-545-4600 or Mr. Lloyd Cluff at 415-973-2791.

Sincerely,

Lawrence F. Womack

SWH/A0597032
Enclosures

cc: Bruce S. Mallett, Region IV
David L. Proulx, Resident
Girija S. Shukla, NRR
Diablo Distribution

San Simeon Earthquake of December 22, 2003

Introduction

On December 22, 2003 at 1116 PST a strong earthquake of moment magnitude (M_W) 6.5 struck the central coast region. The earthquake, called the San Simeon Earthquake, was located approximately 50 km NNW of Diablo Canyon Power Plant (DCPP), in the region 11 km northeast of San Simeon, at a depth of about 7 km. The San Simeon Earthquake is the largest earthquake measured in the San Simeon region. The second largest earthquake in this region was the 1952 Bryson Earthquake of local magnitude (M_L) 6.2, approximately 8 km north of the 2003 epicenter. The San Simeon Earthquake was widely felt from Los Angeles to San Francisco. Earthquake ground effects included landslides and related ground failure near the epicenter, however no surface faulting was observed. Most of the damage occurred in Paso Robles, 39 km ENE of the epicenter. Two deaths have been confirmed due to a building collapse. The earthquake was also strongly felt at DCPP in the Administration Building and the Control Room. Strong motion instruments at the plant site were triggered.

The main shock initiated a rupture at a depth to the southeast and triggered a vigorous aftershock sequence that extends about 30 km southeast of the main shock. As of December 26, 2003, approximately 960 aftershocks have occurred, including about 120 magnitude (M) 3 events and 19 M 4 earthquakes. During the first 24 hours, the activity was about 50 percent higher than the average for a California sequence according to the US Geological Services online report, December 24, 2003, (http://www.usgs.gov/).

The San Simeon Earthquake was a reverse fault event beneath the Santa Lucia Mountains. It occurred along a NW-SE trending fault plane that dips either to the SW or NE. This is a common fault mechanism along this trend. (Reference 1).

Figure 1 shows the location of the main shock and first 20 hours of aftershocks. There is concentrated activity near the main shock and at the southeast end of the aftershock zone. Most of the aftershocks near the main shock are located between the Oceanic and Nacimiento fault zones, whereas the earthquakes to the southeast are not as constrained by the faults. It is not clear which fault, if either, was the cause of the earthquake. The aftershock patterns in depth view (Figure 1, cross sections AA' and BB') show diffuse activity above the main shock and no obvious fault plane. The closest distance from the aftershock zone to DCPP is about 38 km.

Strong Ground Motion

The main shock was felt in the Units 1 and 2 Control Room. It triggered the basic seismic system analog recorder (Kinemetrics SMA) in the Control Room and the Kinemetrics digital recorders (SSA) at the Unit 1 containment base, top of containment, the Auxiliary Building, and the free field pit locations (near the Fitness Trailer). The supplemental system was out of service at the time of the earthquake, however, three temporary accelerometers located in the Auxiliary and Turbine Buildings and a

permanent instrument in the basement of the 500 kV Switching Center triggered. The supplemental system is currently inoperable and replacement parts are obsolete; both the basic and supplemental systems are scheduled to be replaced in January 2004 with new instrumentation.

The earthquake force monitor (EFM) located in the control room measured 0.04g on the horizontal component. The EFM measurement is from the sensor at the Unit 1 containment base and does not have the baseline drift removed. With the baseline shift removed (but prior to filtering), the peak acceleration on the horizontal component is 0.042g. Table 1 lists the peak accelerations, peak velocities and peak displacements of the free-field and Unit 1 containment base ground motions after filtering and baseline corrections are applied. The peak accelerations range between 0.02g and 0.05g, with the largest peak acceleration in the free field, horizontal 2 direction.

Regarding the frequency spectrum, the response spectra were computed for the free-field and Unit 1 containment base recordings. The 5 percent damped spectra for the free-field and Unit 1 containment base recordings are shown in Figures 2 and 3, respectively. The response spectra for this earthquake show a typical spectral shape for rock sites.

For the free-field, both horizontal spectra and the vertical spectra peak at 4 to 5 Hz. These peaks of the free-field spectra are lower than expected for a magnitude 6.5 reverse earthquake recorded at 38 km distance. Current attenuation relations for rock site yield median horizontal spectral accelerations that are 1.5 to 2 times larger than the recorded free-field spectra. For the Unit 1 containment base, the spectra peak at 3 to 4 Hz for all three components. The containment base spectra show amplification in this 3 to 4 Hz range as compared to the free-field spectra. At short frequencies (< 2 Hz), the spectra from the containment base are similar to the free-field spectra. At high frequencies (e.g. 10 Hz), the horizontal spectra from the containment base are smaller than the free-field spectra.

Conclusions

The San Simeon Earthquake is the largest measured in the San Simeon region. The reverse fault motion of the main shock and aftershocks and the aftershock patterns are consistent with previous seismic activity in this region. The free-field ground motions recorded at DCPP are below then median ground motion estimated for this event using current attenuation relations for rock sites.

Dr. Norman Abrahamson and Ms. Marcia McLaren of PG&E Geosciences Department are preparing a detailed report of the San Simeon earthquake. The report will include analyses of the Kinemetrics SMA tape system. The detailed report will be available upon request

Reference

(1) McLaren, M. K. and Savage, W. U. (2000). Seismicity of South-Central Coastal California: October 1987 through January 1997, *Bull Seism. Soc. Am*. 91, no. 6, pp. 1629-1658.

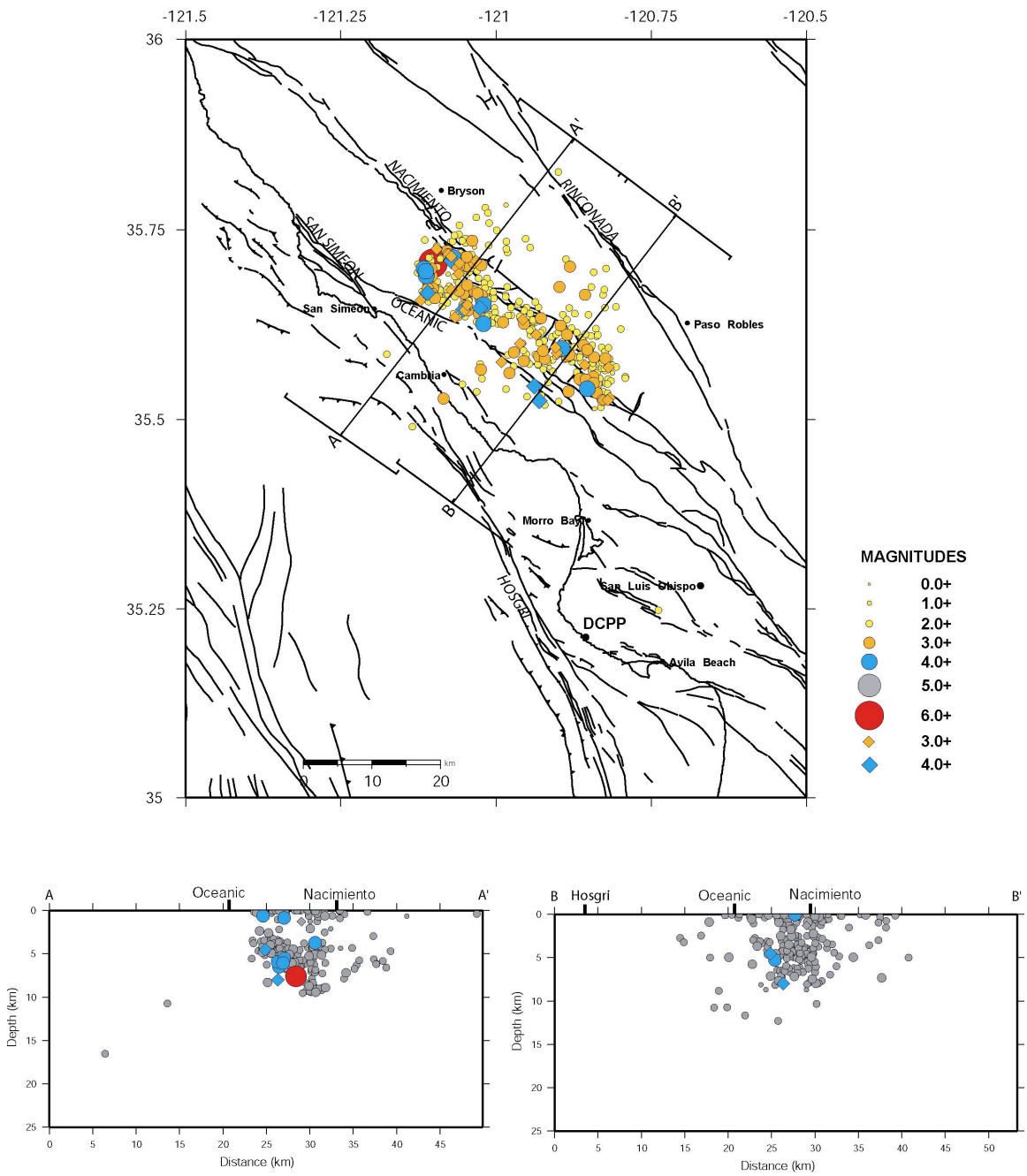

Figure 1. San Simeon Earthquake (large red circle) of 22 December 2003, 19:15 GMT, and aftershocks to 23 December 2003, 14:51 GMT. Nearby faults are labeled. Diamond earthquake symbols are preliminary locations form the USGS website; circles are events that have been reviewed by USGS seismologists NCEDC. Seismicity cross sections AA' and BB' are also shown.

Table 1. Peak ground motions values from the Basic Seismic System digital recorders (after filtering and baseline correction).

Instrument type	Instrument location	Component	Peak Acceleration (g)	Peak Velocity (cm/s)	Peak Displacement (cm)
Kinemetrics SSA	Free field pit (near Fitness Trailer)	Horizontal 1 (Channel 1)	0.034	8.3	7.4
		Vertical (Channel 2)	0.022	7.6	6.3
		Horizontal 2 (Channel 3)	0.046	8.2	4.9
Kinemetrics SSA	Unit 1 Containment base, 89' elev.	Horizontal 1 (Channel 1)	0.033	8.2	7.6
		Vertical (Channel 2)	0.036	8.1	6.3
		Horizontal 2 (Channel 3)	0.041	7.9	5.0

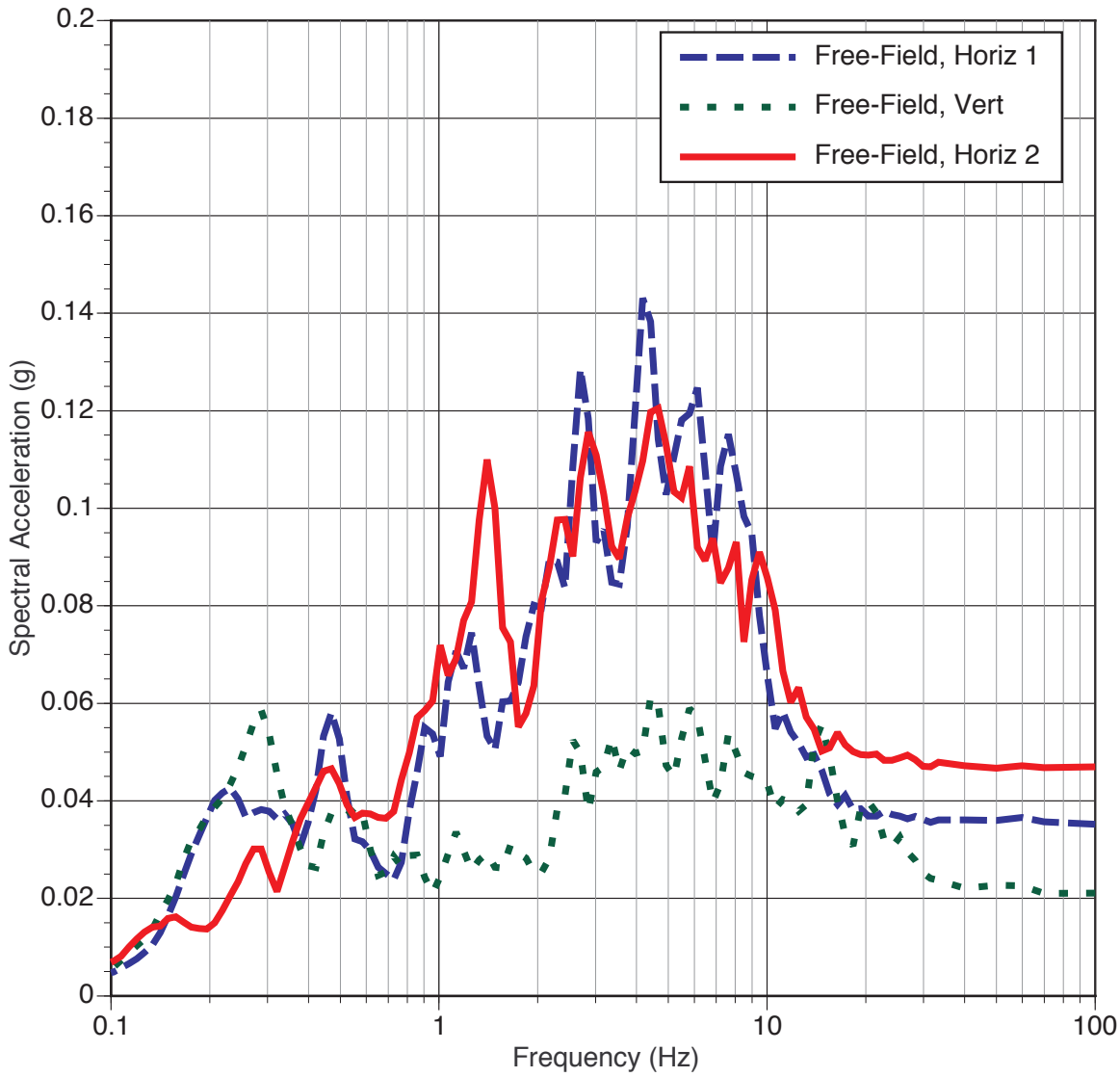

Figure 2. Response spectra at 5% damping for the free-field ground motion.

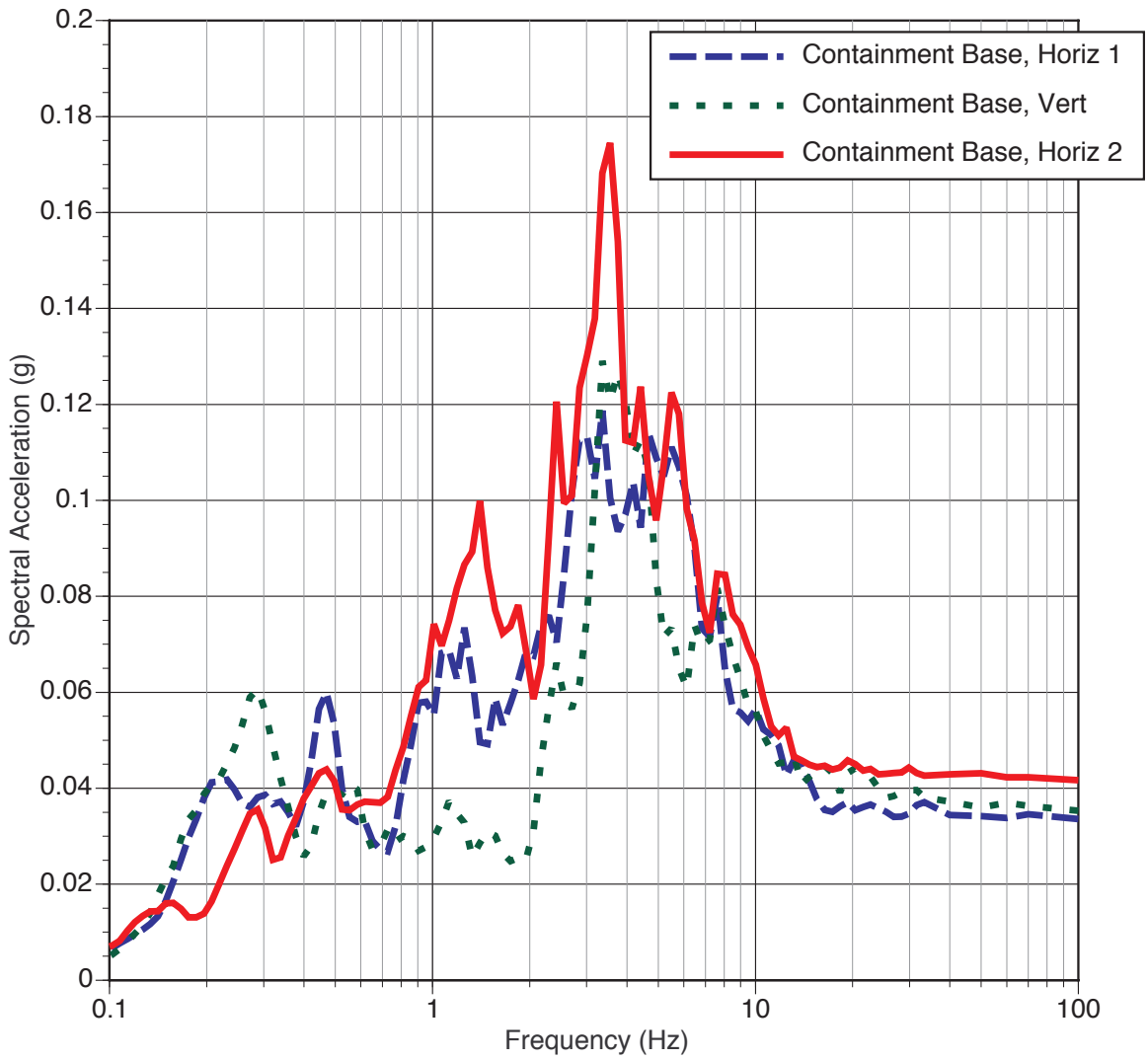

Figure 3. Response spectra at 5% damping for the unit 1 containment base ground motion.

Analysis of The Resultant Effect Upon Facility Features Important To Safety For The San Simeon Earthquake of December 22, 2003

Plant Systems Response:

The San Simeon Eearthquake registered 0.04g at the plant site, as read by the earthquake force monitor (EFM). The duration of the main shock was approximately 22 seconds. During this time, numerous alarms were received on both units. Many of the alarms were associated with movement of fluid levels in various systems. When the seismic activity stopped, the alarms that were received cleared and returned to normal. Operations responded by dispatching people into the power plant to visually verify systems that had received level alarms. Examples of the level alarms include; spent fuel pools, electro-hydraulic (EH) control system, and startup transformer 1-1. Operations took action to restore the operation of the Unit 2 EH pumps that had tripped off line due to a low-low system level lockout. This low-low system level lockout was due to the motion of the EH fluid; there were no leaks from the system. All other investigations to alarms revealed no leakage from systems and no damage caused by the earthquake. It was noted that the seismically-induced wave action in the Unit 1 spent fuel pool was of sufficient magnitude to cause a small amount of water to splash up onto the surrounding deck of the pool. Plant personnel were dispatched to clean this area.

Per Casualty Procedure (CP) M-4, “Earthquake,” a walkdown of the facility was conducted. All systems continued to operate normally. No visible damage was discovered. Operations personnel performed inventory checks required by CP M-4; no systems were found to be leaking as a result of the earthquake. DCPP Fire Department personnel conducted plant walkdowns, including both containment structures to verify the continued integrity of fire protection features. No observable damage was discovered within the power plant and containment structures. No fire protection impairments were found. Operations personnel also performed an inventory of the diesel fuel oil storage tanks. No abnormalities were observed.

Seismic Monitoring Instrumentation Response:

The main shock triggered the basic seismic system analog recorder (Kinemetrics SMA) in the Control Room and the Kinemetrics digital recorders (SSA) at the Unit 1 containment base, top of containment, the Auxiliary Building, and the free-field pit locations (near the Fitness Trailer). The supplemental system was inoperable at the time of the earthquake, however, three temporary accelerometers located in the Auxiliary and Turbine Buildings and a permanent instrument in the basement of the control room at the 500 kV Switching Center triggered. The EFM located in the Control Room measured 0.04g on the horizontal component

All functional seismic monitoring instrumentation operated as designed.

OUTGOING CORRESPONDENCE SCREEN
(Remove prior to NRC submittal)

Document: PG&E Letter DCL-03-184

Subject: Special Report 03-04**:** San Simeon Earthquake of December 22, 2003

File Location: S:\RS\RA\Report\Specials\DCL03184 Special Report 12.22.2003 Earthquake.doc

FSAR Update Review
Utilizing the guidance in XI3.ID2, does the FSAR Update need to be revised? Yes [ ] No [x] If "Yes", submit an FSAR Update Change Request in accordance with XI3.ID2 (or if this is an LAR, process in accordance with WG-9)

Commitment #1: NONE

Clarification:

Appendix L-3

Mw 6.0 Parkfield Earthquake of September 28, 2004

Mw 6.0 Parkfield Earthquake of 28 September 2004

Preliminary Report by Geosciences Department, PG&E

A (Mw 6.0) earthquake occurred Tuesday, September 28, 2004 at 10:15:24 PDT at a depth of 8 km (5 miles) near Parkfield, California (Figure 1). This is the long-awaited Parkfield earthquake. It is the seventh in a series of repeating earthquakes that have occurred on the Parkfield section of the San Andreas fault at fairly regular intervals in 1857, 1881, 1901, 1922, 1934, and 1966. The first in 1857, was a foreshock to the great Fort Tejon earthquake (Mw 7.9), which ruptured the fault from Parkfield to the southeast for over 180 miles. In 1984 the USGS "predicted" the next Parkfield (M 6.0) earthquake would take place within the time window of 1988 to 1993, therefore, the September 28 earthquake was at least ten years behind the expected occurrence. The six (M6.0) earthquakes are termed "characteristic" because they all ruptured the same area on the fault and were about the same magnitude. This September 28 earthquake ruptured the same region as the 1966 event and fits the description of a characteristic Parkfield earthquake. Strong shaking lasted about 10 seconds. The aftershocks extend along the San Andreas fault from 5km SE of the epicenter to about 25 km NW of the epicenter, at the SE end of the creeping (aseismic) section of the fault.

The 2004 earthquake was located by the California Integrated Seismograph Network (CISN) at 35.815N, 120.374W. This location is 7 miles SSE of Parkfield, and 50 miles NE of DCPP (Figure 1 inset). As of October 5, over 900 aftershocks have been recorded, including two M5 and five M4 events. The two M5.0 events occurred on 9/29 at 10:19 PDT and on 9/30 at 11:54 PDT at about 10 km depth. Both locate to the northwest, 12 and 15 miles, respectively, from the main shock. The CISN focal mechanisms from the main shock and aftershocks indicate the events occurred on a northwest trending right-lateral strike-slip fault (Figure 2), consistent with motion along the San Andreas fault. Surface rupture of a few cms has been observed at various locations along the fault between the section of the fault 15 km SE of the epicenter to 20 km NW of the epicenter near the 9/29 M5.0 aftershock (Figure 1).

Figure 3 shows maps of the shear stress calculations for the 1983 Coalinga earthquake (Mw 6.2) and the 2003 San Simeon earthquake (Mw 6.5). These results suggest that the Coalinga earthquake may have retarded the Parkfield earthquake (Parkfield section in blue, low shear stress zone), while the San Simeon earthquake may have ratcheted up the stress at Parkfield 9 months ago (Parkfield section in red, high stress change zone; Ross Stein, personal communication).

The earthquake was strongly felt in the Parkfield area. No deaths or injuries have been reported to date. The San Miguel Substation was the closest PG&E facility to the event, 18 miles to the west. No damage was reported. Figure 1 shows that the 500 kV and 230 kV electric transmission lines and the line 306 Gas transmission line cross the fault within about 5 km of the epicenter. PG&E made field checks and no damage was reported. The earthquake was felt at DCPP (eg. the Administration building), but was not felt in the control room at the site. The newly installed Consolidated Seismic System

recorded the earthquake on all 19 instruments. The data are summarized below in the Strong Motion section.

Strong Ground Motion

In anticipation of the Parkfield earthquake, this part of the San Andreas fault is particularly well instrumented due to the presence of the CISN Parkfield array (Figure 4). Consequently, there are many strong motion recordings of the earthquake. Although the aftershock patterns are predominantly from the epicenter to the NW, the recorded ground motions are highly variable, suggesting that slip along the fault was complex.

A key feature of the near-fault ground motions is the large variability: near the fault the average horizontal peak accelerations range from 0.1 to 1.3g. The closest station to the epicenter was about 3 km to the NW; it recorded 0.16 g. The highest acceleration of 1.3 g was at the northern end of the aftershock zone, north of Parkfield, about 15 km from the epicenter. Two additional stations recorded over 1 g ground motions, within 5 km of Parkfield. These recordings are near the location of the two M5 aftershocks. There also was unusually strong ground shaking recorded southeast of the epicenter, suggesting that the rupture was not unilateral. A peak acceleration of 0.85 g was recorded 9 km SE of the epicenter, less than 1 km from the fault, and two additional stations to the SE and E of the fault recorded accelerations of 0.84 g and 0.82 g.

The free-field peak accelerations recorded at DCPP are compared to other free-field peak acceleration in Figure 5. The distance from DCPP to the Parkfield rupture is about 85 km. This comparison shows that the peak accelerations recorded at DCPP are slightly smaller than other peak acceleration at similar rupture distances. Also shown in this figure are the peak accelerations predicted by the Abrahamson & Silva (1997) attenuation relation for a magnitude 6.0 strike-slip earthquake. Since all the site conditions are not currently available, both rock and soil attenuation relations are shown. Overall, the Abrahamson and Silva model is consistent with the observed PGA values, but it tends to overestimate the peak accelerations at large distances.

DCPP Strong Ground Motion

The main shock was felt in the DCPP Administration building and it triggered the newly installed Consolidated Seismic System (CSS). The location of the new CSS are listed in Table 1 and are shown in Figures 6 and 7**.**

The recordings were processed as follows:

1. Remove the baseline shift.
   The average acceleration over the first two seconds was used to remove the baseline shift.

2. Determine useable frequency band
   The Fourier spectra of the recordings were computed. Based on the shape of the Fourier spectra, the reliable frequency band was estimated. For free-field recordings, high-pass corner frequencies of 0.1 Hz and 0.2 Hz were selected

for the horizontal and vertical components, respectively. For the in-structure recordings, high-pass corner frequencies of 0.2 Hz and 0.4 Hz were selected for the horizontal and vertical components, respectively. For all components, low-pass corner frequencies of 40 Hz were selected.

3. Apply a band-pass filter
   Using the corner frequencies identified in step 2, a band-pass filter is applied to each recording. A 5-pole Butterworth filter is used.

4. Apply baseline correction
   A baseline correction is applied to the band-pass filtered recordings. The displacement baseline is modeled using a high-order polynomial without the constant or linear terms.

5. Integrate to velocity and displacement
   The baseline corrected recordings are then integrated to velocity and displacement using a time domain integration. The normalized arias intensity (used to compute the duration) is also computed in this step.

6. Compute the response spectra
   In the final step, the response spectra at 5% damping are computed.

Table 1 lists the peak accelerations, peak velocities, and peak displacements of the recordings from the Consolidated Seismic System. The free-field ground motions had peak horizontal accelerations of about 0.006g to 0.011g after the baseline shift, filters, and baseline corrections are applied. The peak vertical accelerations on the free-field recordings were less than one-half of the average horizontal peak acceleration.

The acceleration, velocity, and displacement time series for the three-components of free-field station ESTA28 are shown in Figures 8-10. The normalized Arias intensity, shown in Figure 11, is used to evaluate the duration of the ground shaking. One common measure of duration is the time interval from the 0.05 to 0.75 level of the normalized Arias Intensity (called the 5-75% duration). For these recordings, the 5-75% duration corresponds to about 7 seconds.

The free-field response spectral values at frequencies greater than 1 Hz recorded at the DCPP site were factors of 2-3 lower than the median response spectral values computed for this earthquake using attenuation relations similar to those used in the LTSP (Figure 12). This is partly due to the general over-prediction of the ground motions at large distances by the attenuation relation and partly due to the larger than typical shear-wave velocities at DCPP (the DCPP site has a shear-wave velocity of 4500-5000 ft/s, but the attenuation relations used in the LTSP were based on ground motions primarily recorded on soft-rock and shallow soil sites with shear wave velocity of about 1500-2000 ft/s). Sites with larger shear-wave velocities tend to have smaller ground motions since there is less of an impedance contrast.

The 5% damped response spectra for all the CSS recordings are shown in Figures 13 to 31.

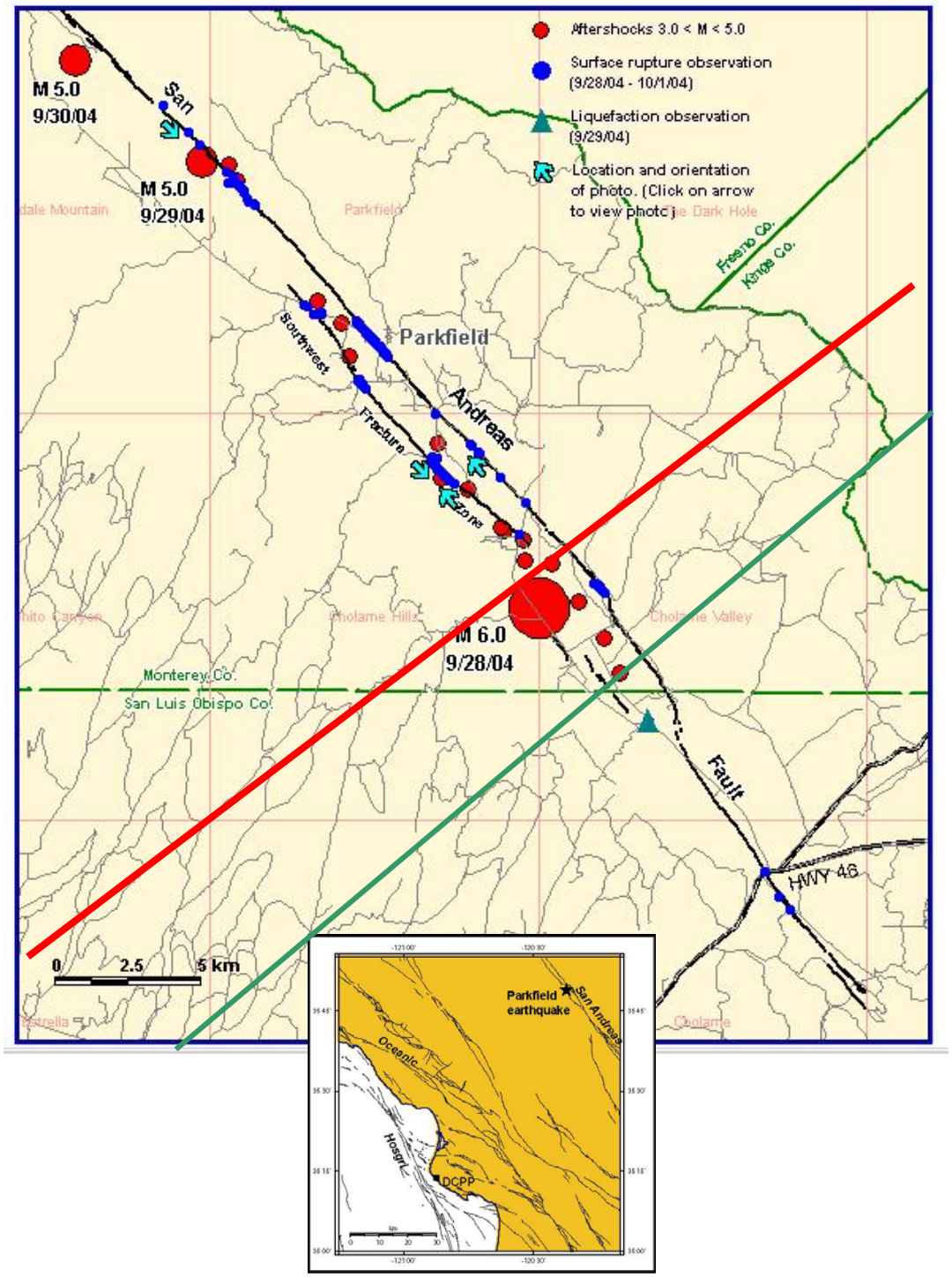

Figure 1. Location of the September 28, 2004 Parkfield earthquake (Mw6.0). Also shown are M3 and greater aftershocks, surface rupture observations, and locations of the 500/230kV transmission lines (red line) and the Gas pipeline 306 (green line). Inset map shows earthquake with regional faults.

```
September 28, 2004 at 17:15:24 UTC ML=6.0; (USGS/UCB

Berkeley Moment Tensor Solution

Best Fitting Double-Couple:
   Mo = 9.82E+24 Dyne-cm
   Mw = 5.96
   Z  = 8. km



                  ------
            ------------ P ----
         ##-------------   -------
       ####-------------------------
      #######--------------------------
     #########-------------------------#
    ###########----------------------####
   #############------------------#######
   ##############--------------##########
  ################-----------#############
  #################-------################
  ###################-----##################
  ####################--################
  #################----################## T
   #############---------################
   ##########-------------################
    ######----------------##############
     #----------------------############
      ------------------------#########
        -----------------------######
          -----------------------##
            -------------------
                  -------
```

Figure 2. USGS moment tensor focal mechanism for the Mw 6.0 Parkfield earthquake

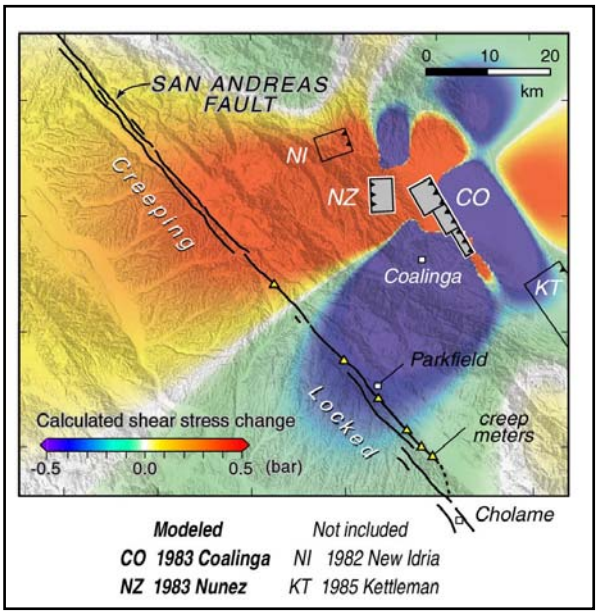

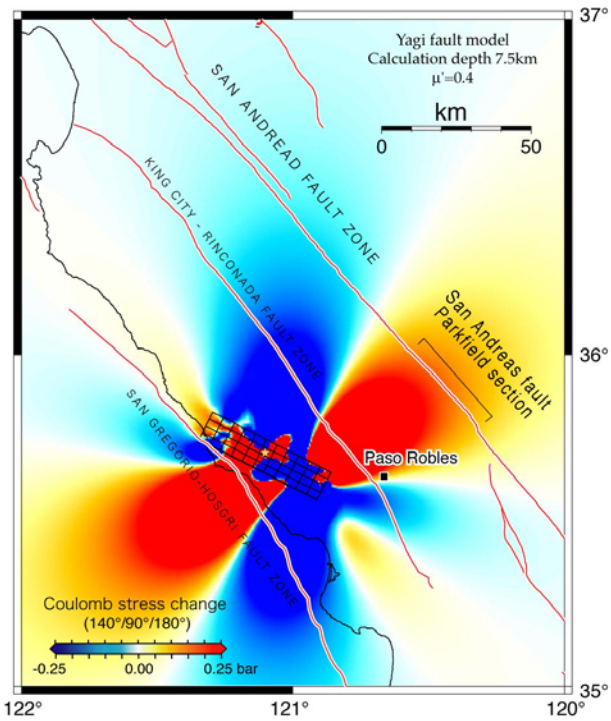

Figure 3. Top figure is the calculated shear stress imposed by the 1983 Coalinga earthquake on planes parallel to the San Andreas fault at 8 km depth; bottom figure is calculated shear stress from the 2003 San Simeon earthquake. (Figures from Ross Stein, US Geological Survey, 10/7/04)

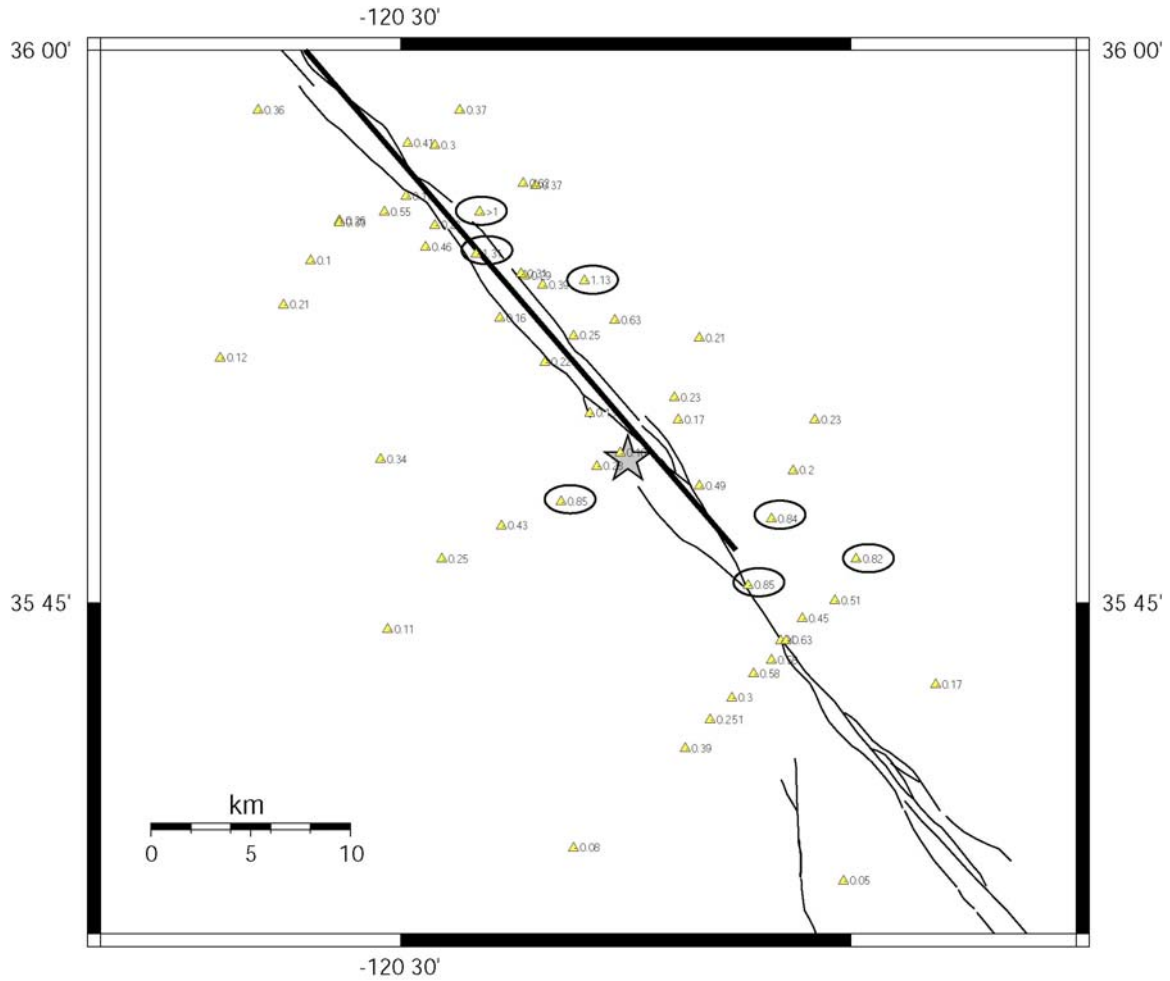

Figure 4. Location of the CISN strong motion instruments with corresponding peak horizontal ground motions. Values greater than 0.80g are circled. The heavy line shows the rupture dimension used for computing the rupture distances.

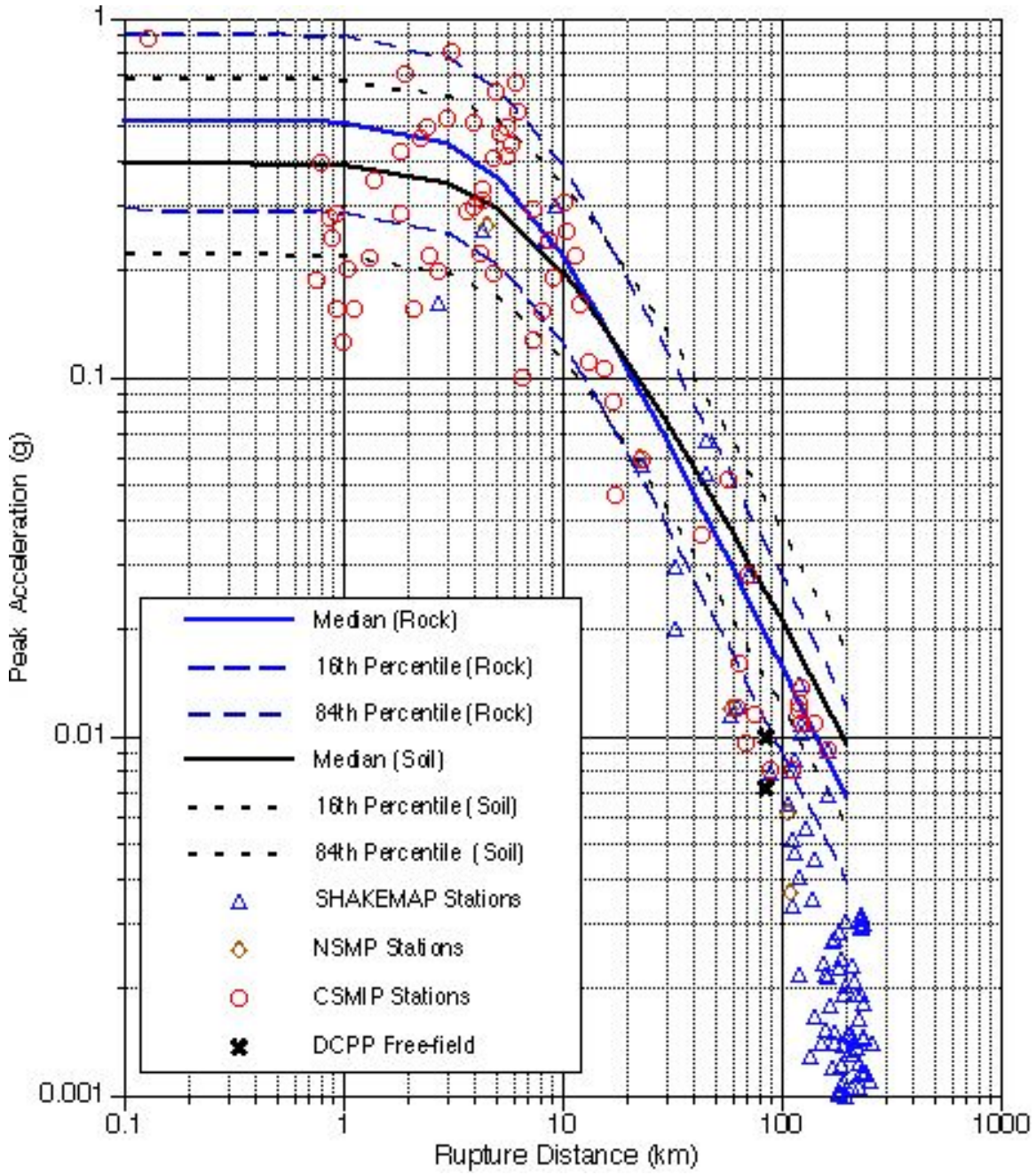

Figure 5. Peak accelerations for the average horizontal component recorded during the Parkfield earthquake compared with the Abrahamson and Silva (1997) attenuation relation. Both rock and soil curves are shown since the site classifications were not yet reviewed.

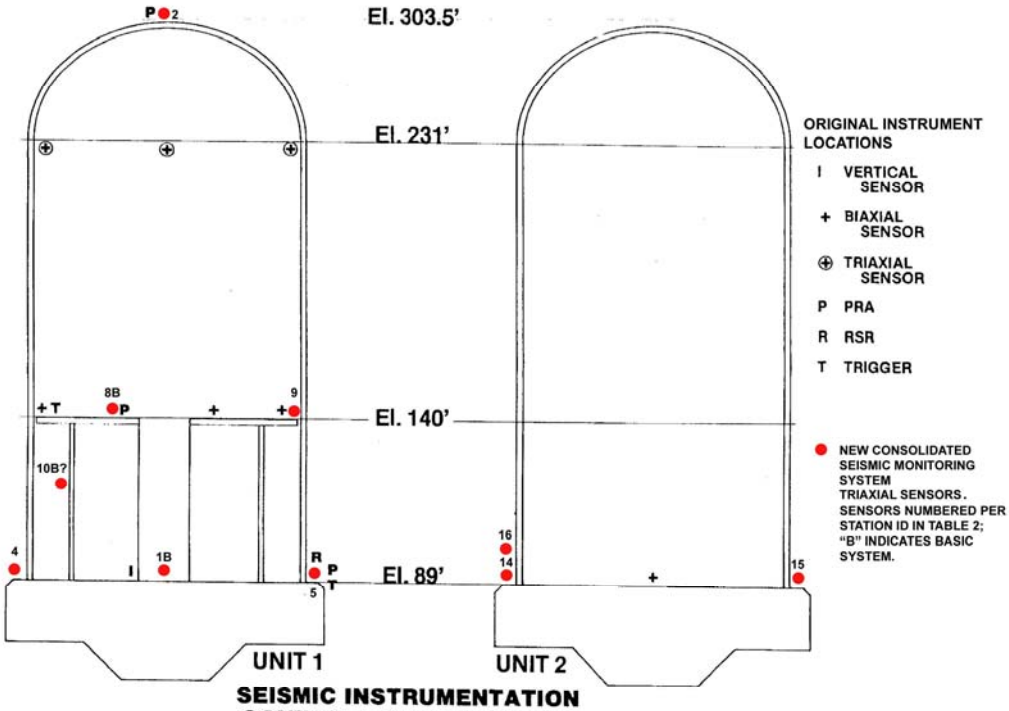

SEISMIC INSTRUMENTATION
CONTAINMENT STRUCTURE
DIABLO CANYON UNITS 1 & 2
FIGURE 1

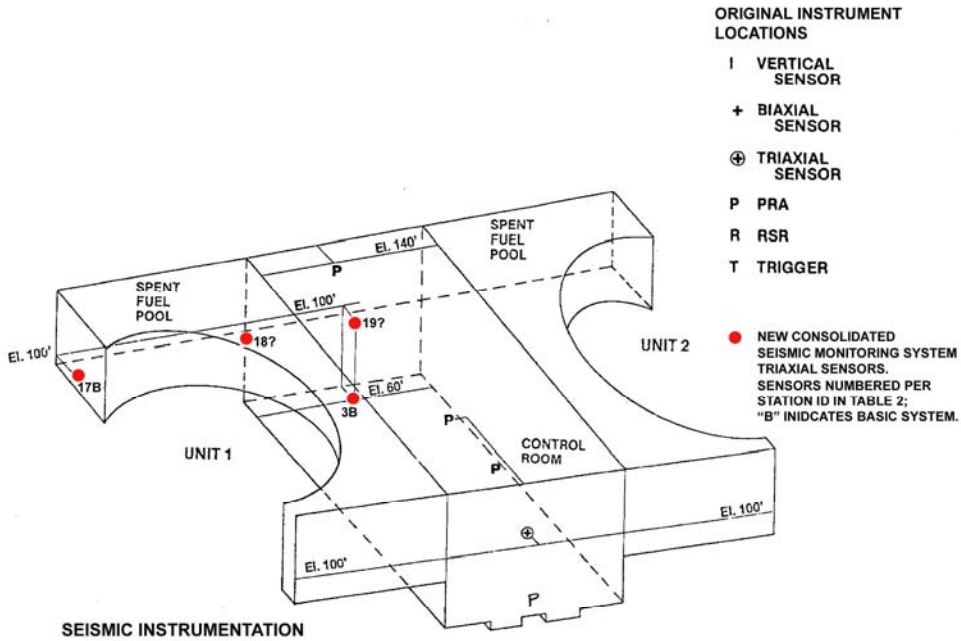

SEISMIC INSTRUMENTATION
AUXILIARY BUILDING
DIABLO CANYON UNITS 1&2
FIGURE 2

Figure 6. Location of Consolidated Seismic System instruments in Units 1 and 2 Containment (top) and Auxiliary building (bottom).

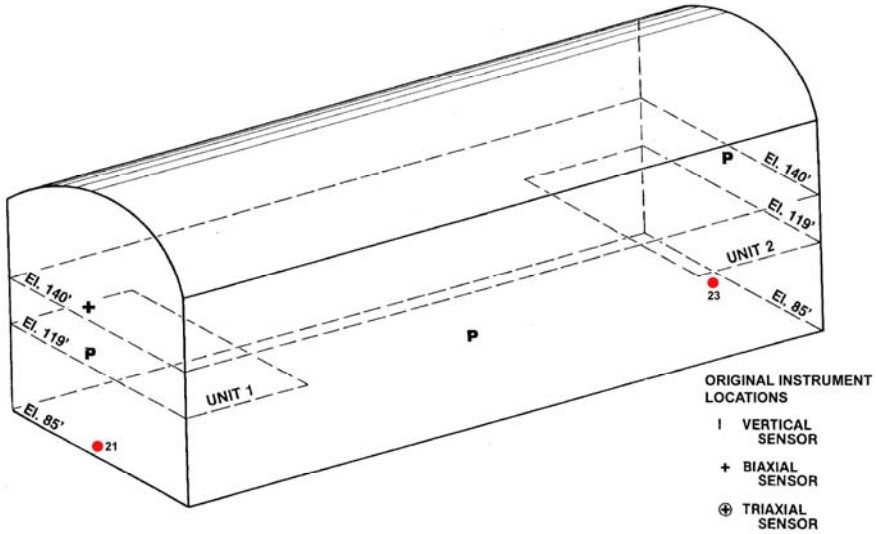

ORIGINAL INSTRUMENT LOCATIONS

- I VERTICAL SENSOR
- + BIAXIAL SENSOR
- ⊕ TRIAXIAL SENSOR
- P PRA
- R RSR
- T TRIGGER
- ● NEW CONSOLIDATED SEISMIC MONITORING SYSTEM TRIAXIAL SENSORS. SENSORS NUMBERED PER STATION ID IN TABLE 2; "B" INIDCATES BASIC SYSTEM.

SEISMIC INSTRUMENTATION
TURBINE BUILDING
DIABLO CANYON UNITS 1 & 2
FIGURE 3

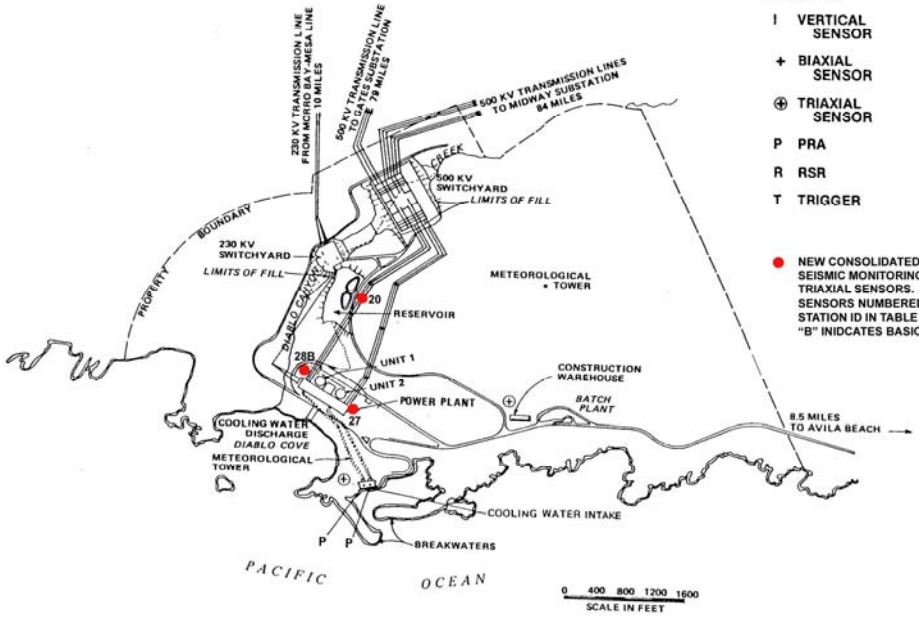

ORIGINAL INSTRUMENT LOCATIONS

- I VERTICAL SENSOR
- + BIAXIAL SENSOR
- ⊕ TRIAXIAL SENSOR
- P PRA
- R RSR
- T TRIGGER
- ● NEW CONSOLIDATED SEISMIC MONITORING SYSTEM TRIAXIAL SENSORS. SENSORS NUMBERED PER STATION ID IN TABLE 2; "B" INIDCATES BASIC SYSTEM.

UNITS 1 AND 2
DIABLO CANYON SITE
SEISMIC INSTRUMENTATION
FIGURE 4

Figure 7. Location of Consolidated Seismic System instruments in Units 1 and 2 turbine building (top) and Free field (bottom).

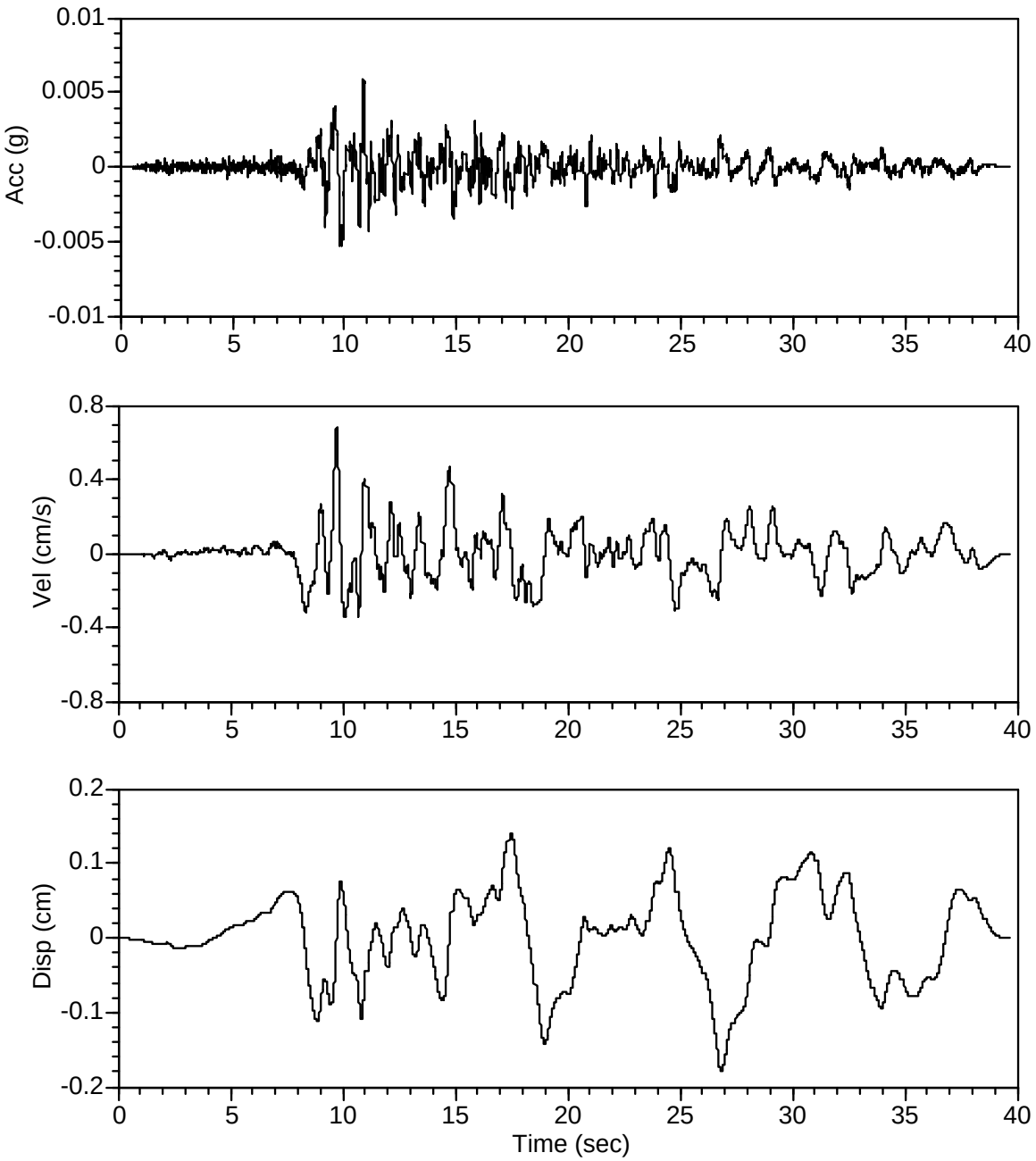

Figure 8. Free-field ground motions: ESTA28 X component (85' elev. Free Field in paved area north of U1 containment).

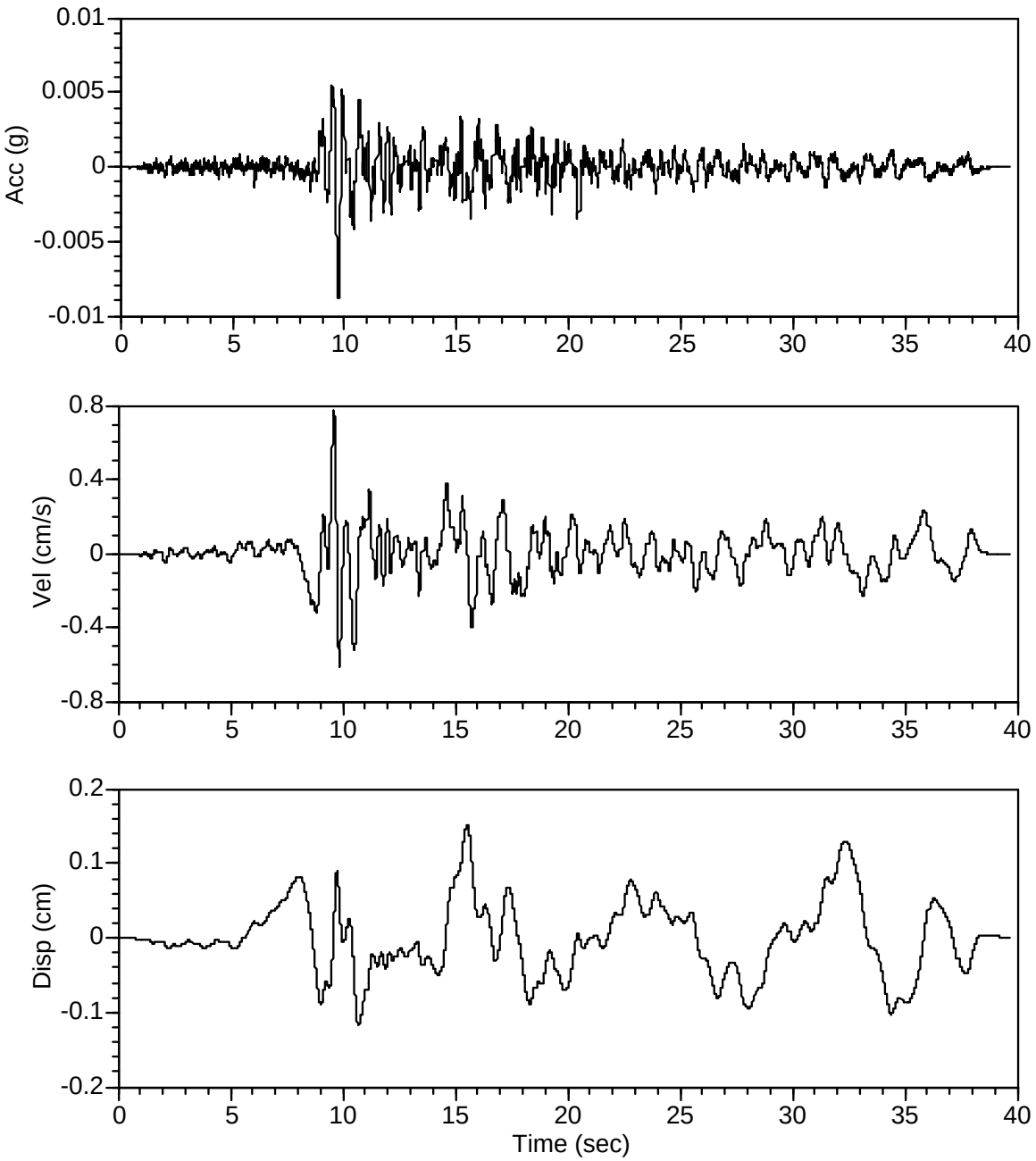

Figure 9. Free-field ground motions: ESTA28 Y component (85' elev. Free Field in paved area north of U1 containment).

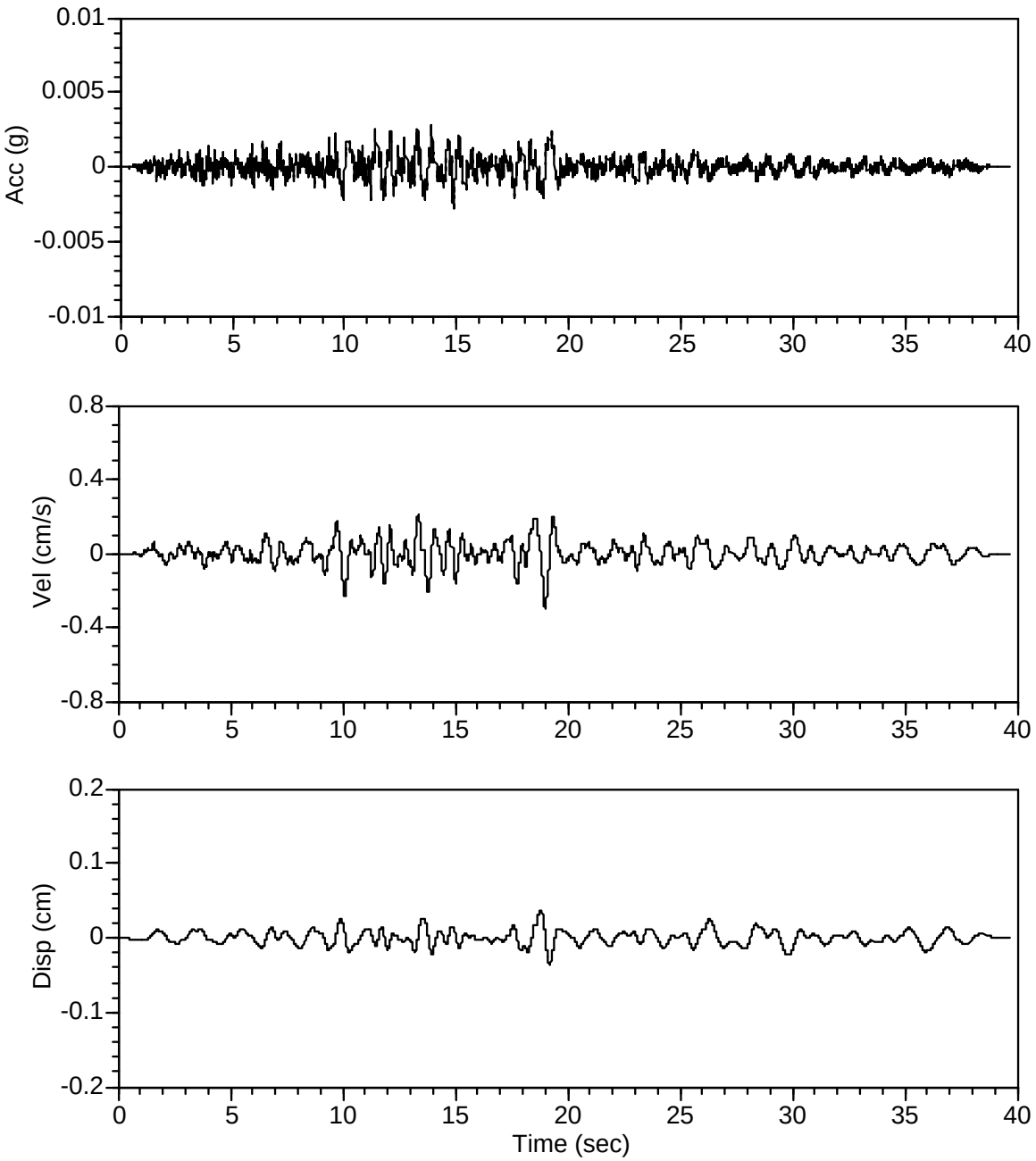

Figure 10. Free-field ground motions: ESTA28 Z component (85' elev. Free Field in paved area north of U1 containment).

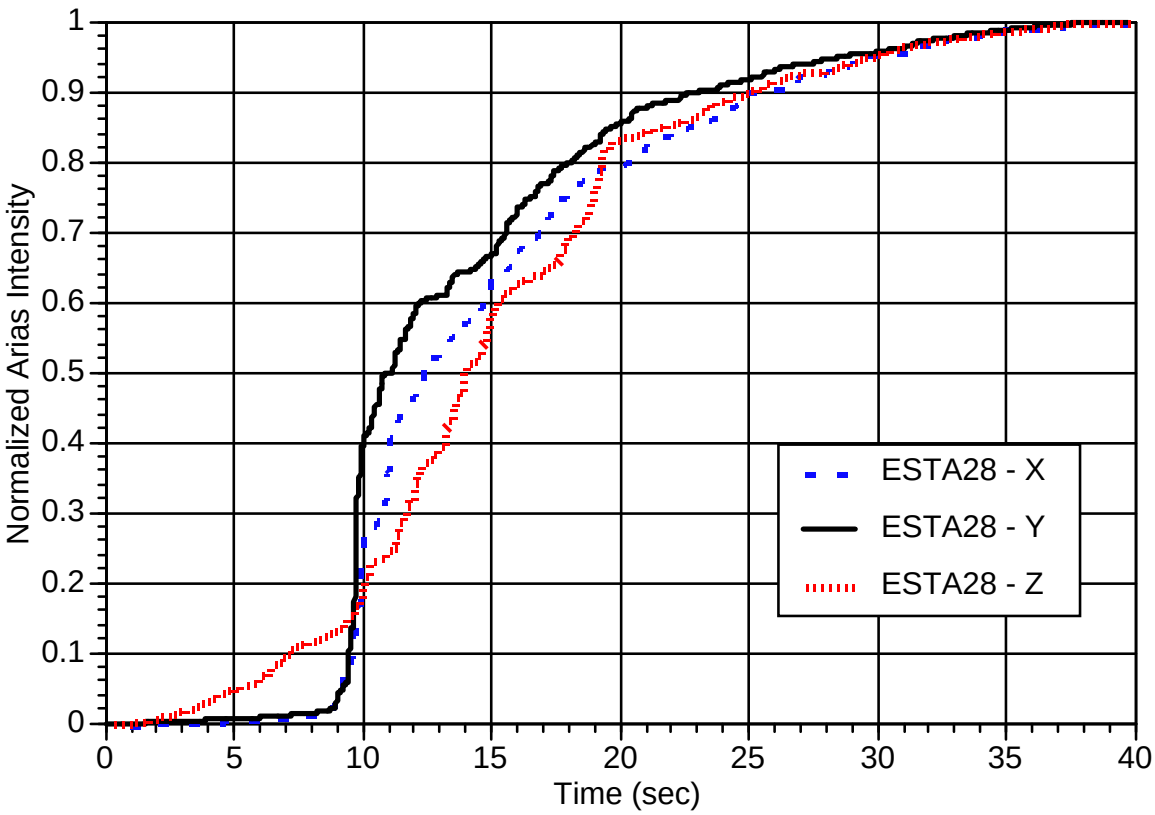

Figure 11 Acceleration normalized Arias Intensity from free-field station ESTA28. This shows the duration of the accelerograms.

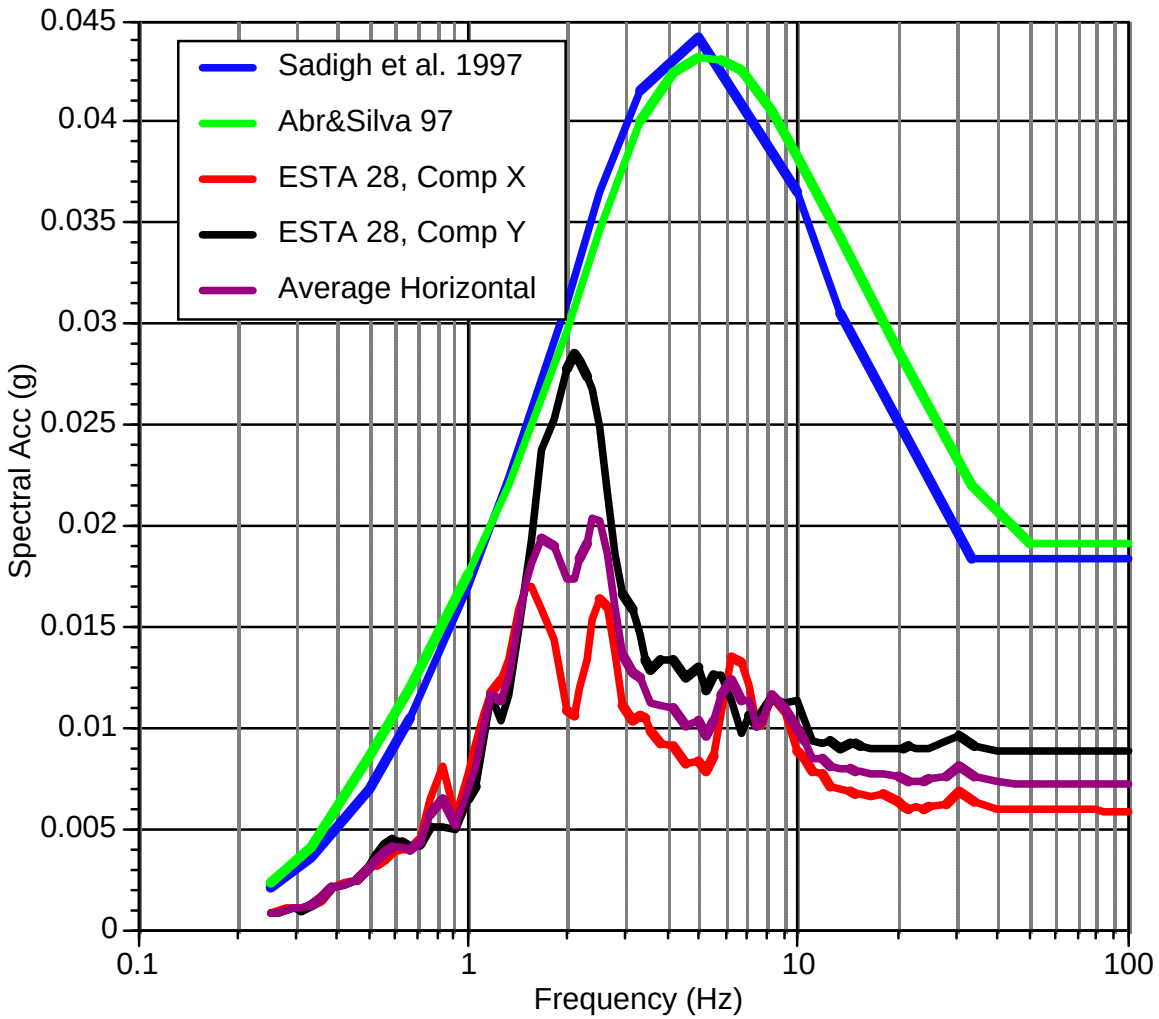

Figure 12. Comparison of free-field spectra from DCPP with those predicted from commonly used attenuation relations.

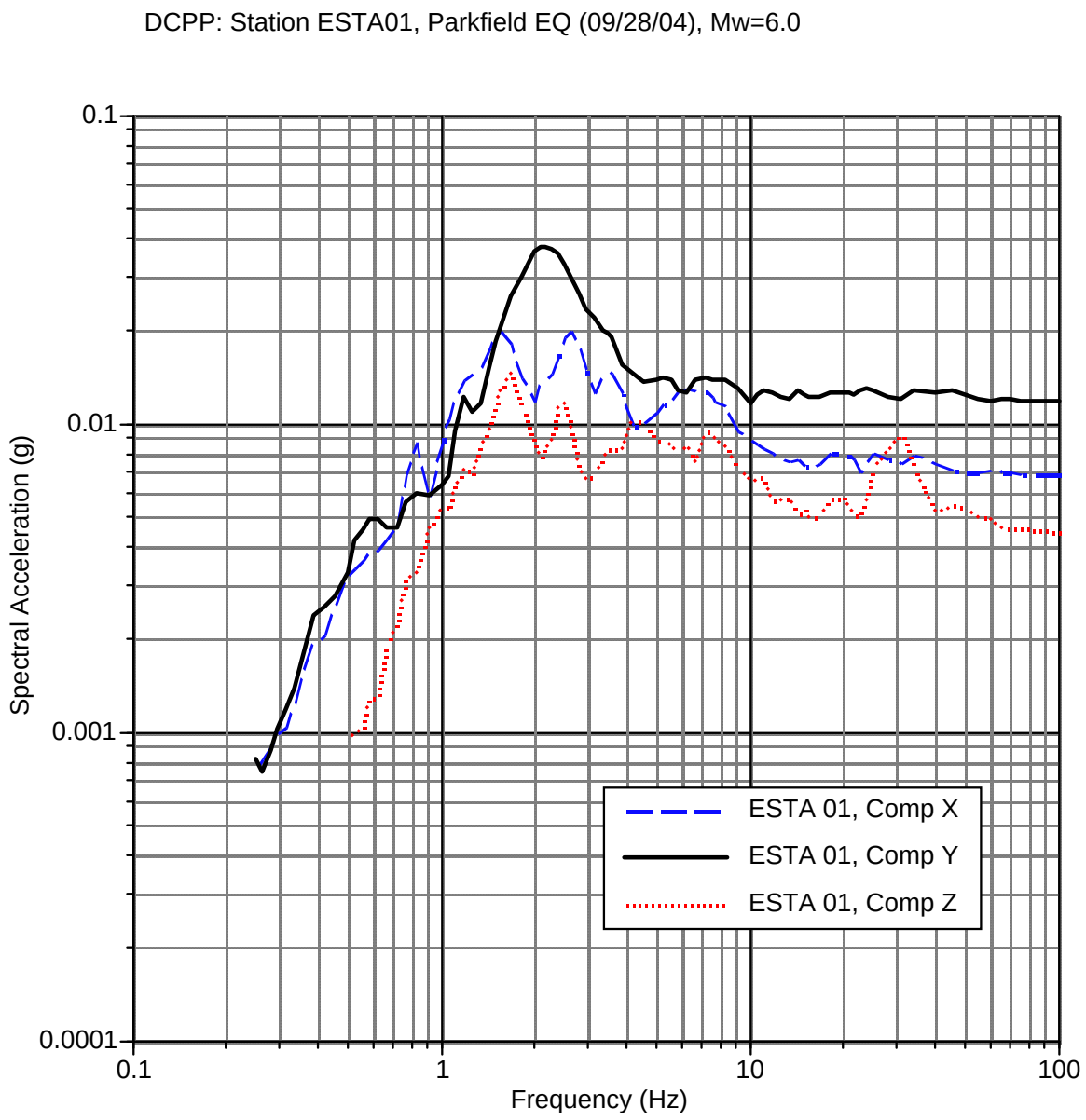

Figure 13. Response spectra at 5% damping for ESTA 01 (89', 180 degrees on containment Base Slab).

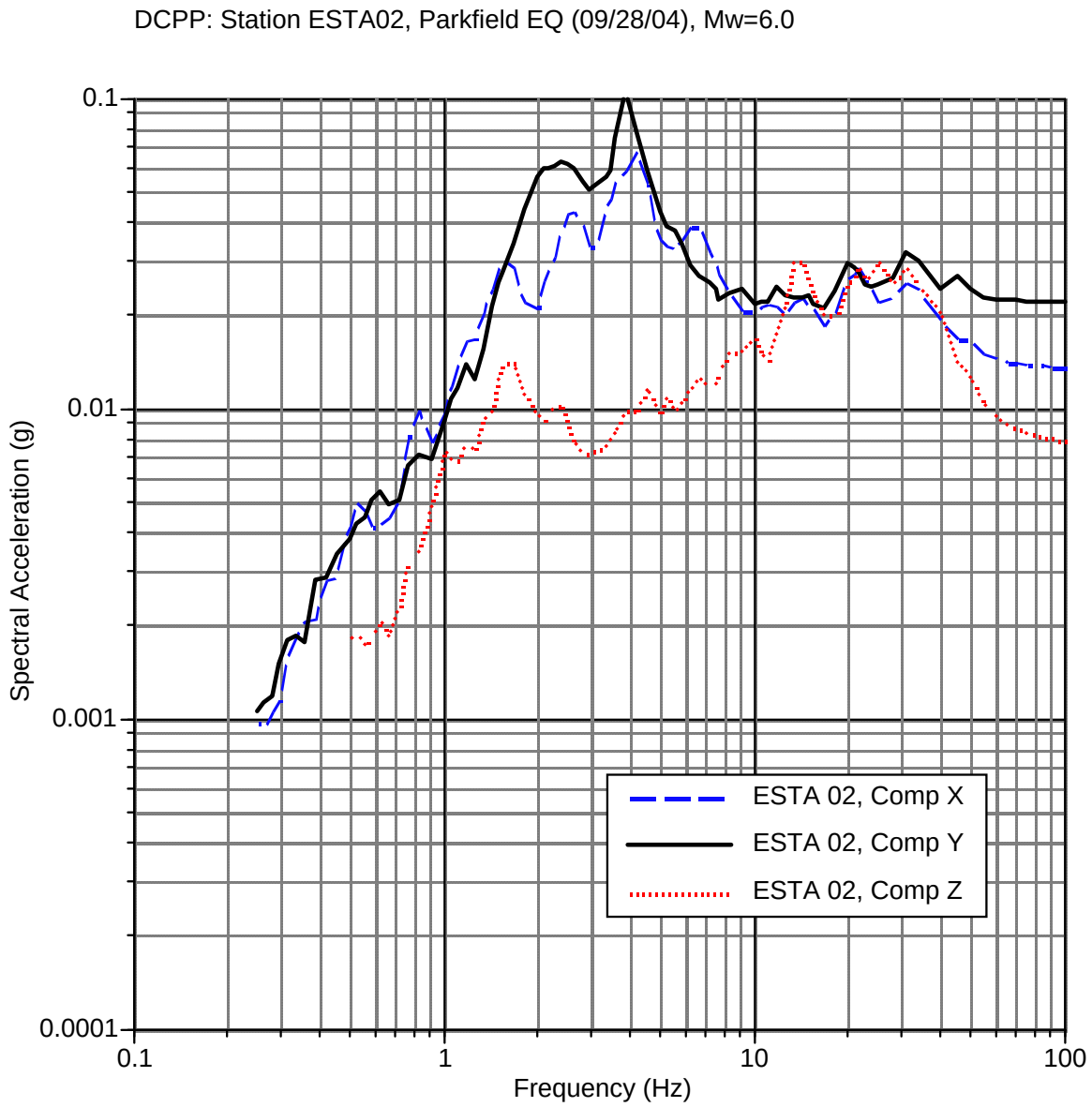

Figure 14. Response spectra at 5% damping for ESTA 02 (U1 303' elevation, 225 degrees).

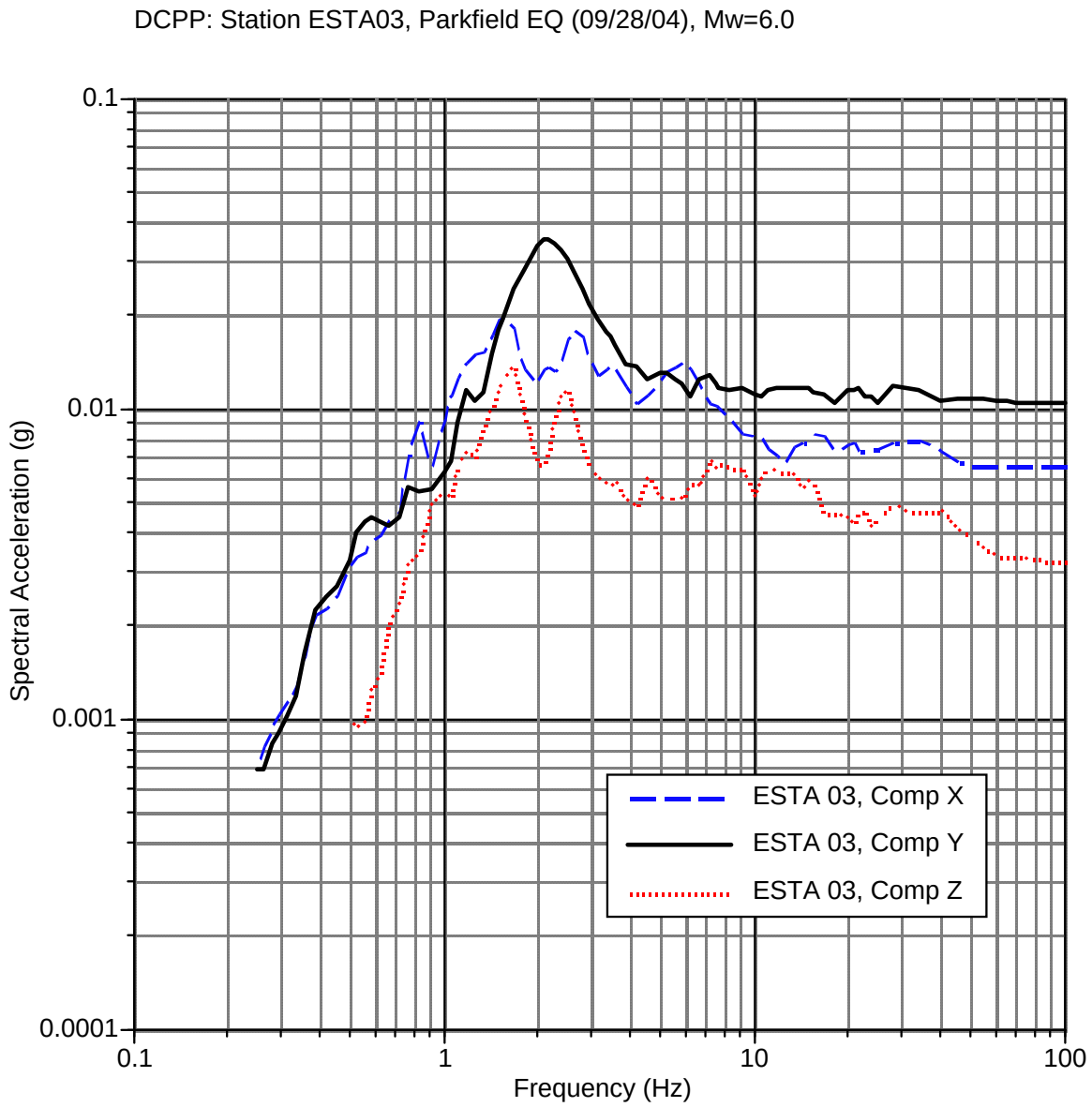

Figure 15. Response spectra at 5% damping for ESTA 03. (64' elev, U1 in Aux. Bldg).

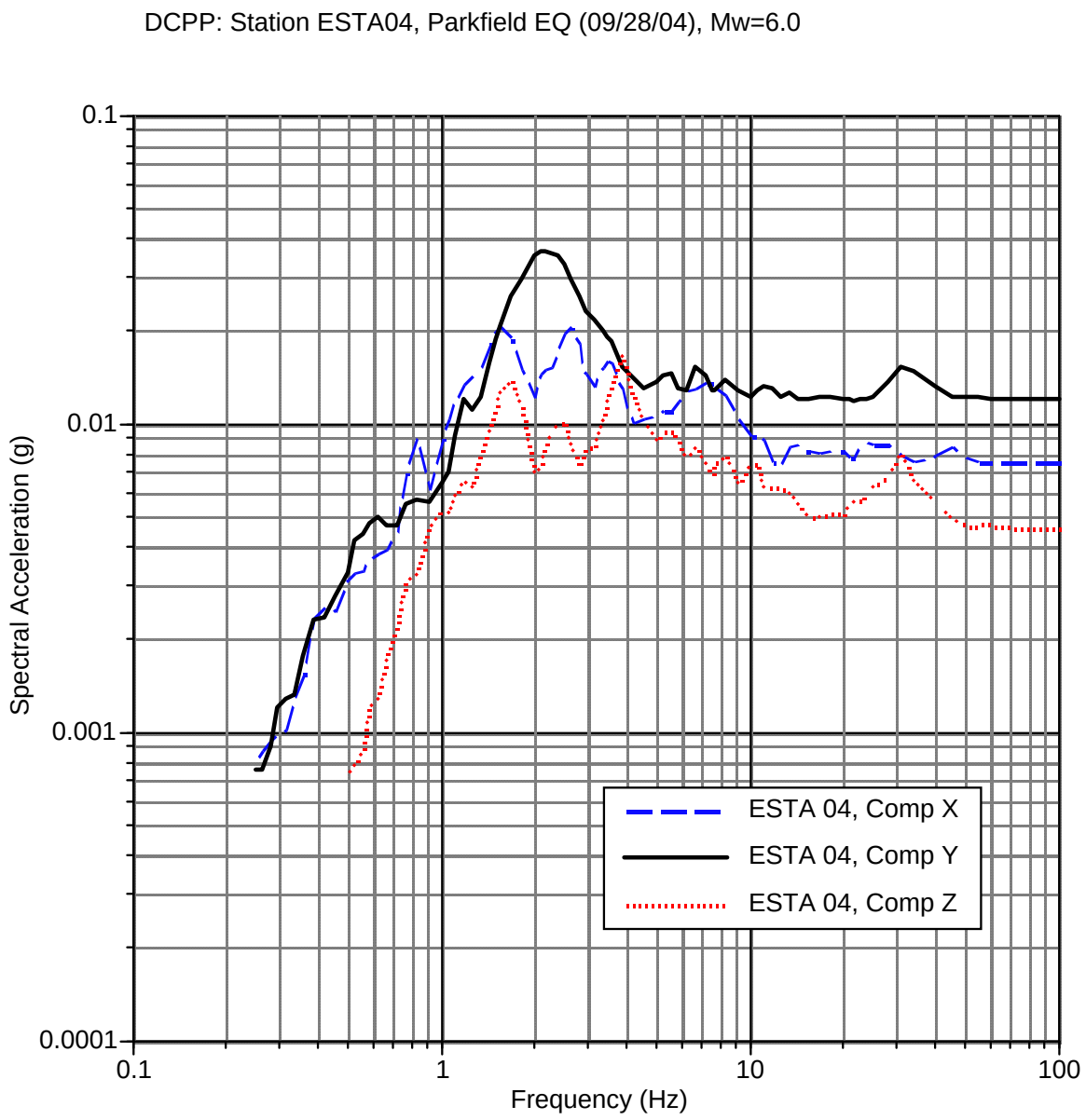

Figure 16. Response spectra at 5% damping for ESTA 04 (89' elev, area FW outside U1 containment on Base Slab).

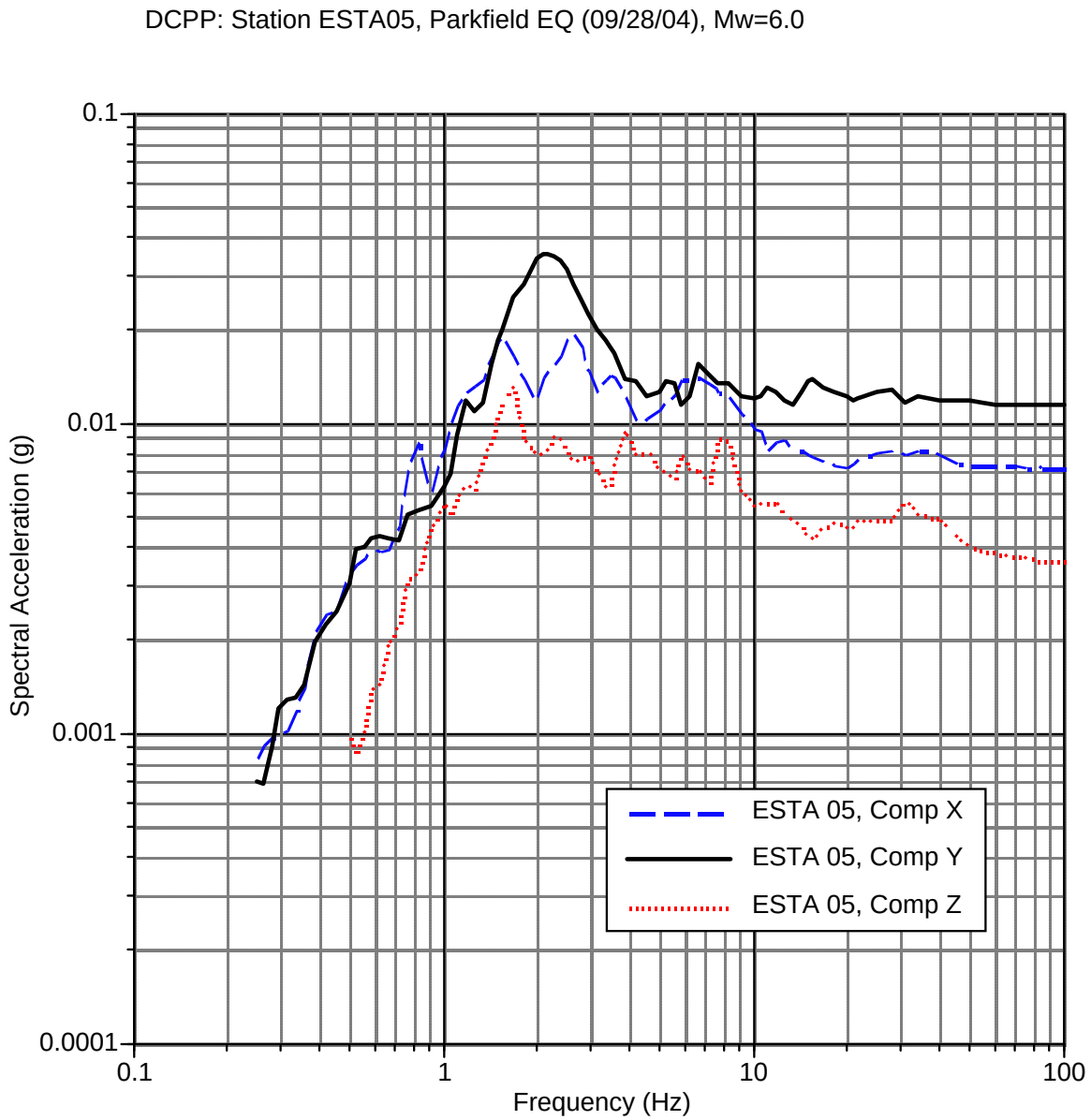

Figure 17. Response spectra at 5% damping for ESTA 05(89' elev, outside U1 containment on Base Slab).

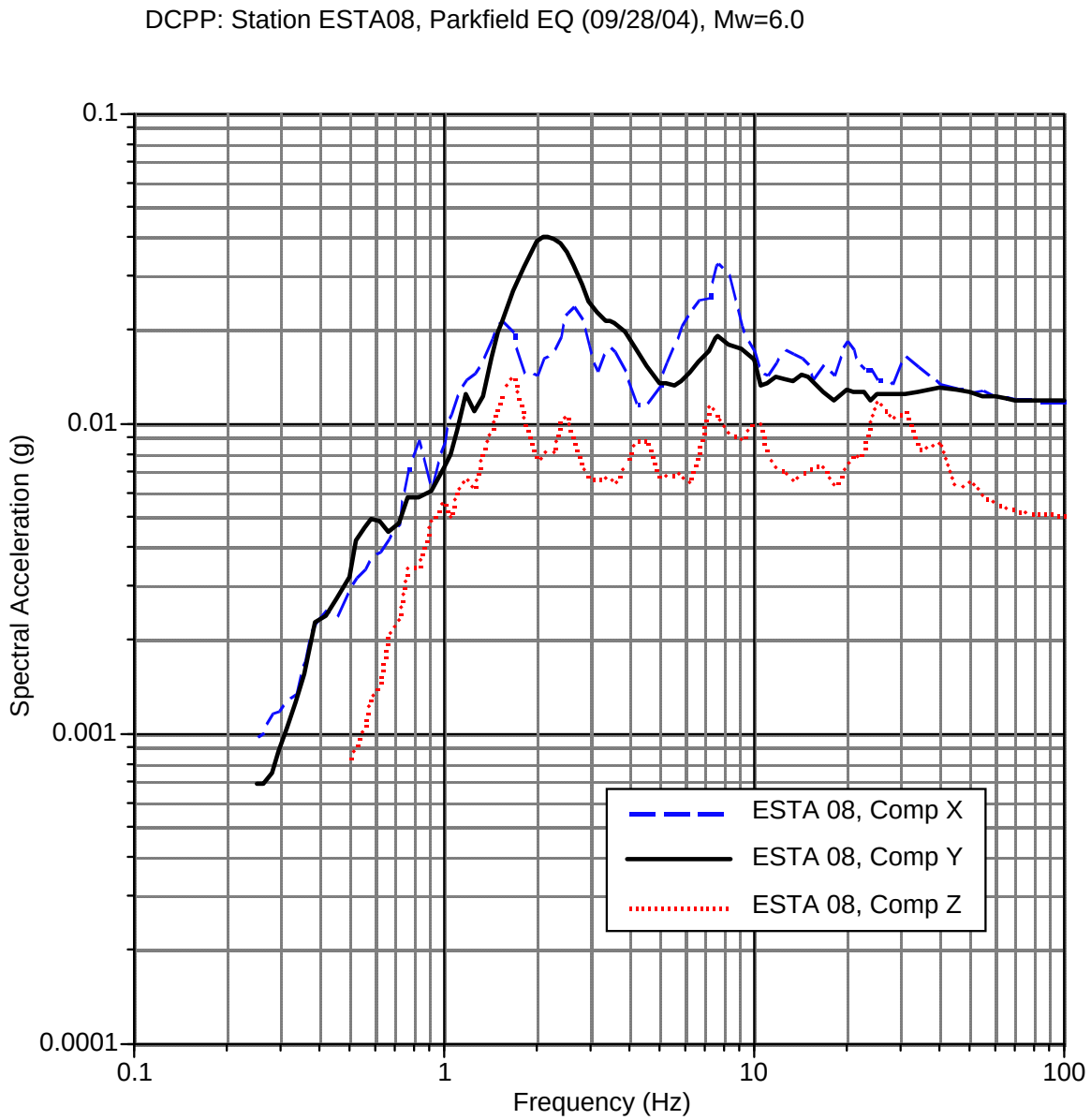

Figure 18. Response spectra at 5% damping for ESTA 08 (140' elev in U1 containment at operating floor).

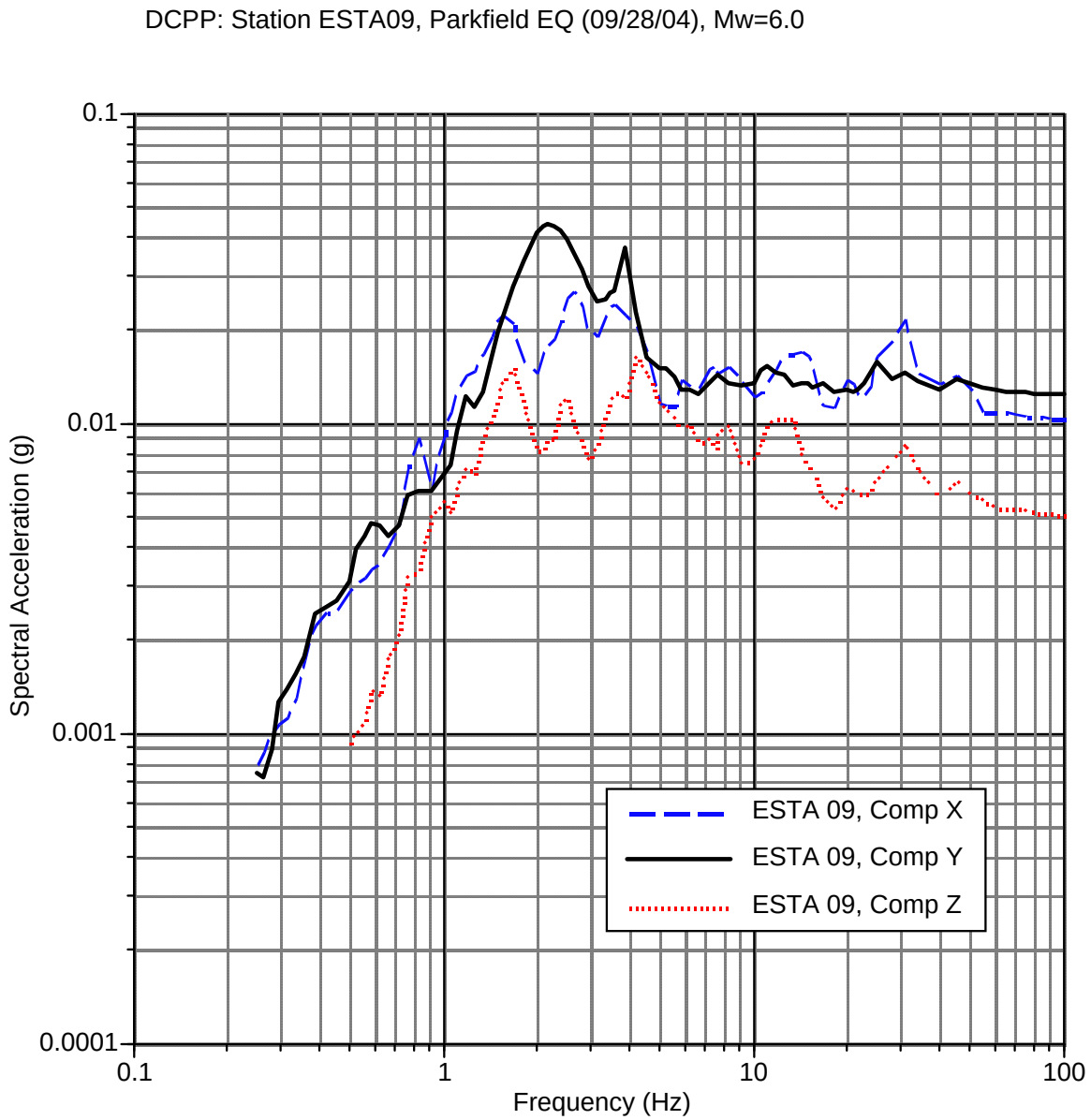

Figure 19. Response spectra at 5% damping for ESTA 09 (140' elev in U1 containment on liner).

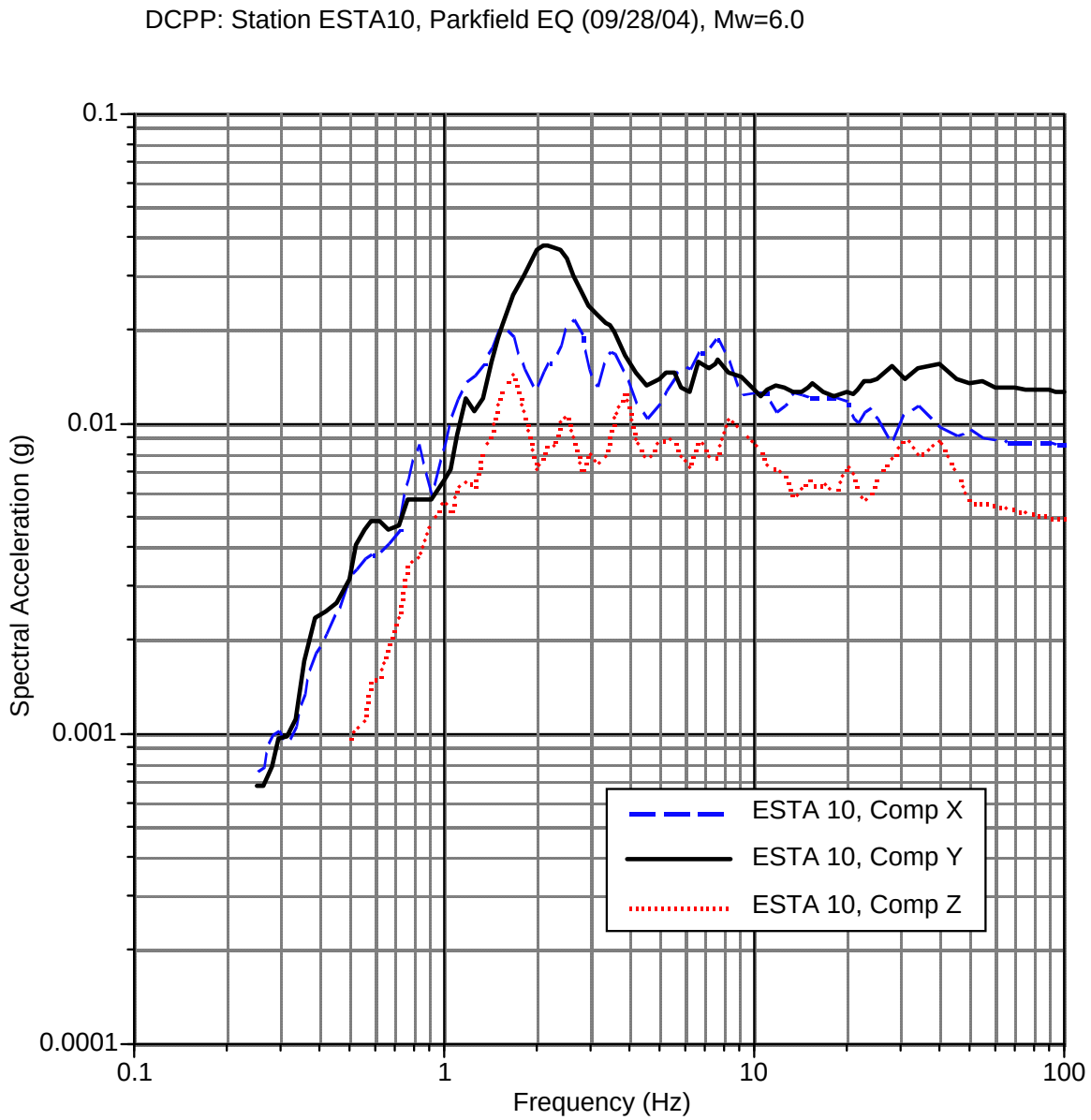

Figure 20. Response spectra at 5% damping for ESTA 10 (117' elev in U1 containment on bio shield).

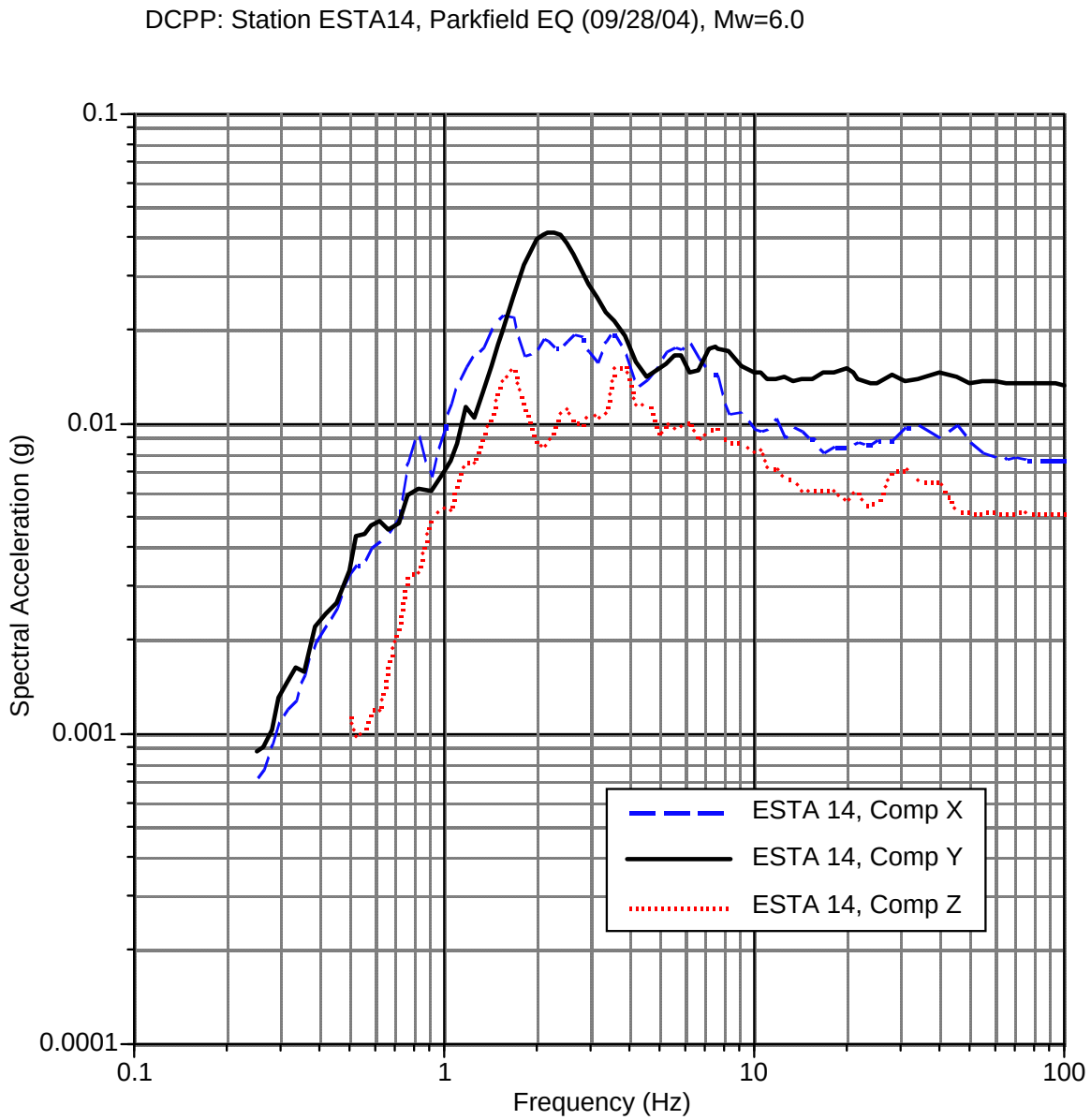

Figure 21. Response spectra at 5% damping for ESTA 14 (89' elev outside U2 containment on base slab).

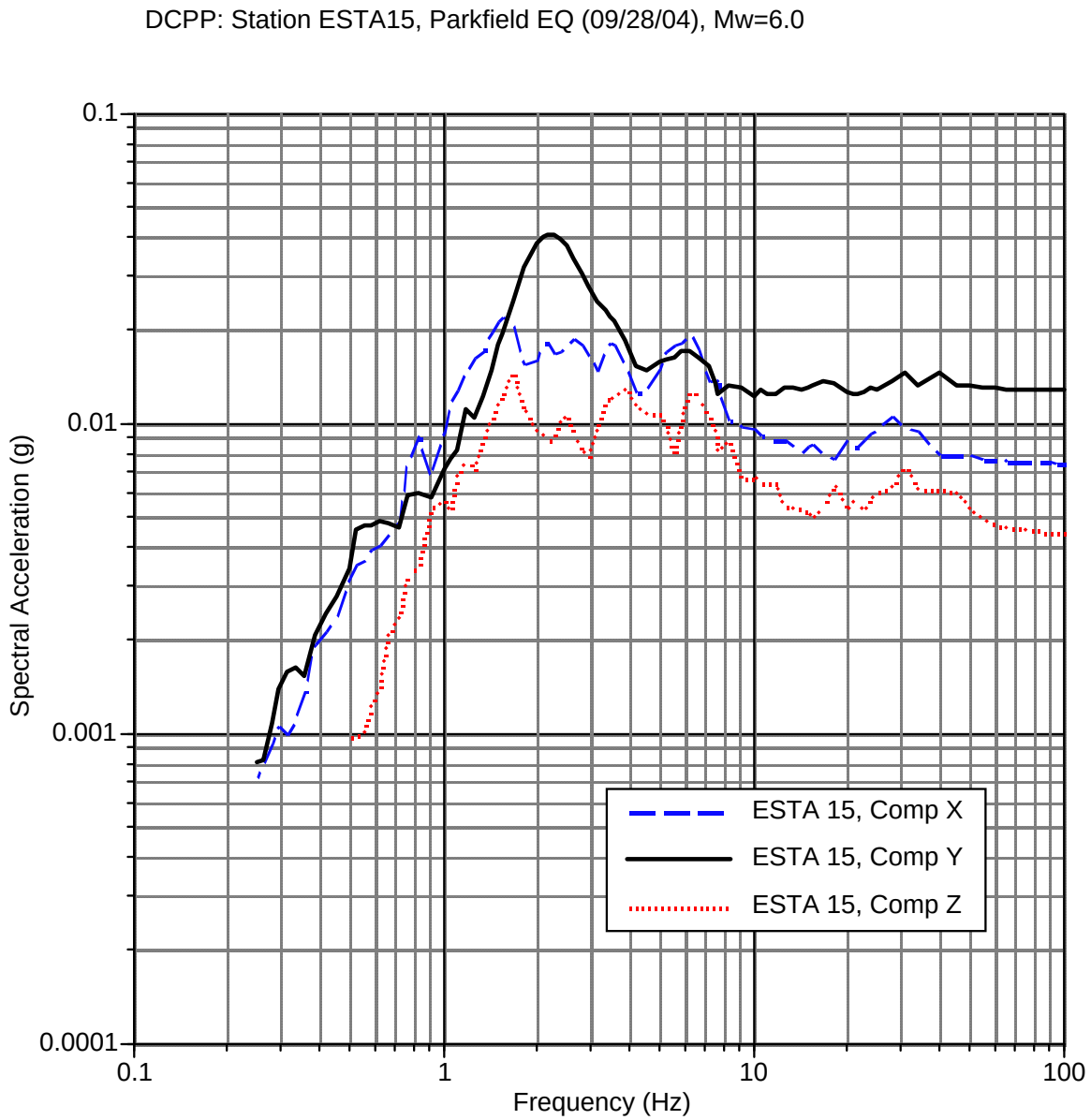

Figure 22. Response spectra at 5% damping for ESTA 15 (89' elev outside U2 containment on base slab).

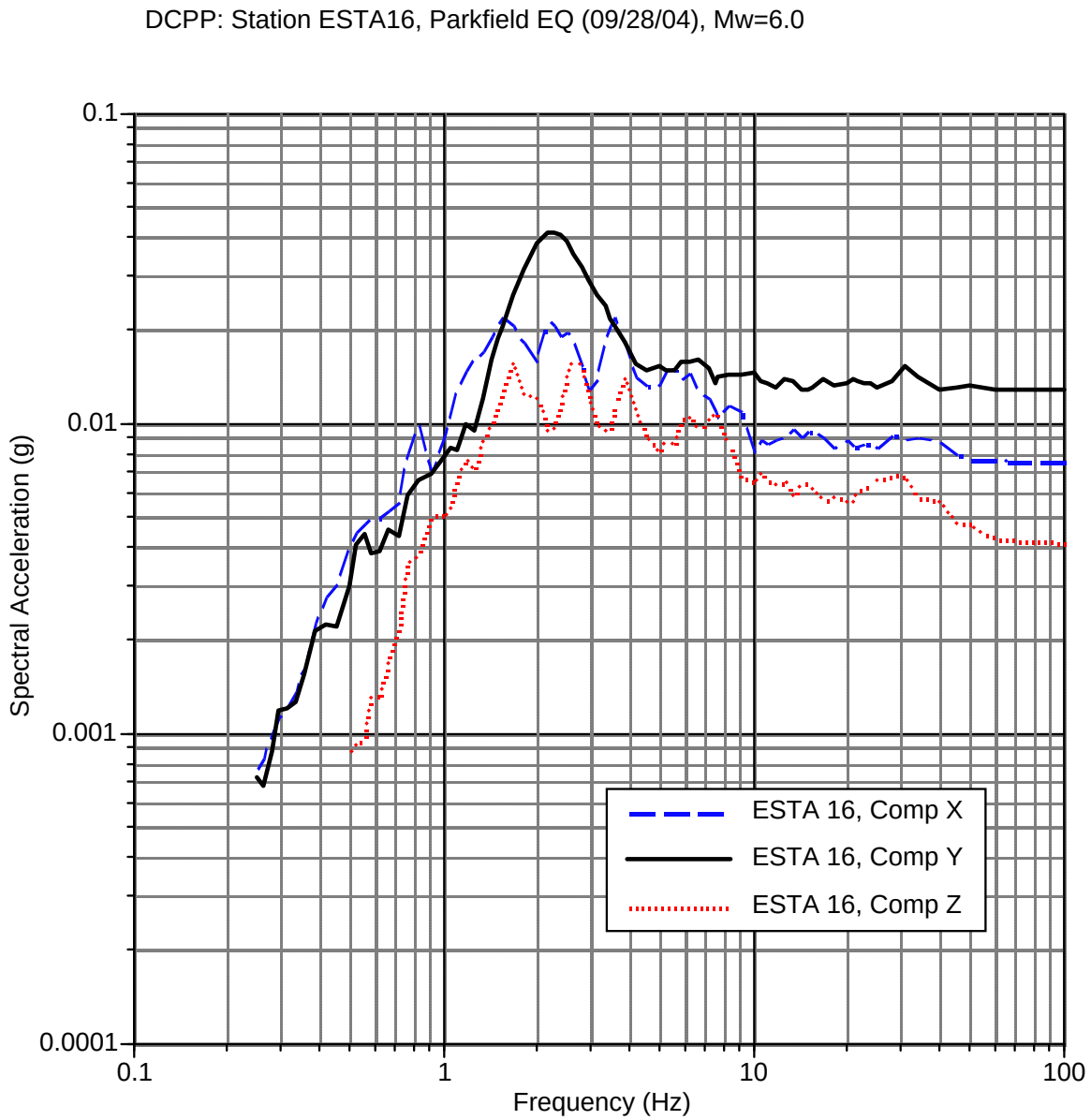

Figure 23. Response spectra at 5% damping for ESTA 16 (89' elev outside U2 containment on base slab).

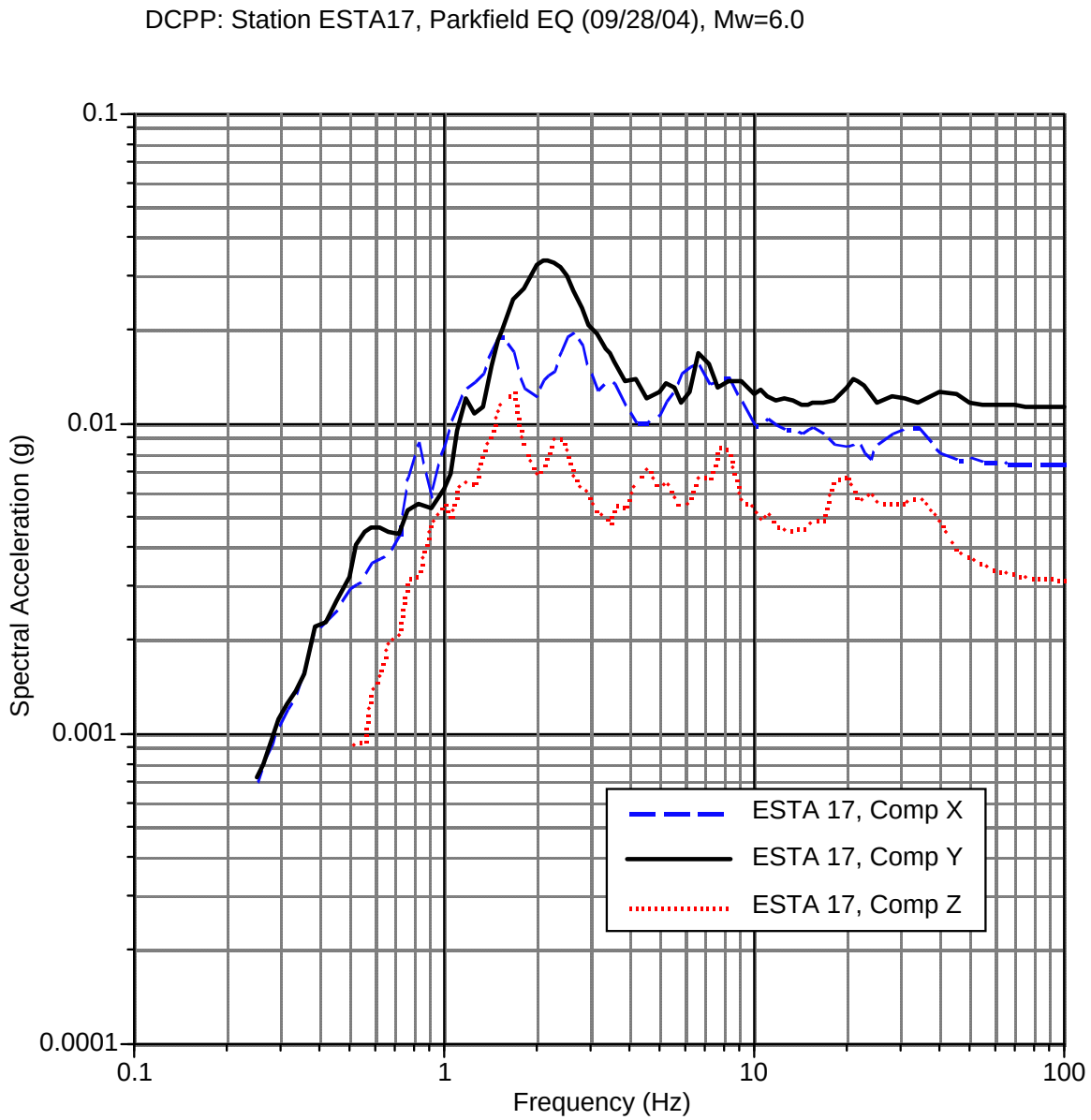

Figure 24. Response spectra at 5% damping for ESTA 17 (100' elev U1 Aux/Fuel Handling Building).

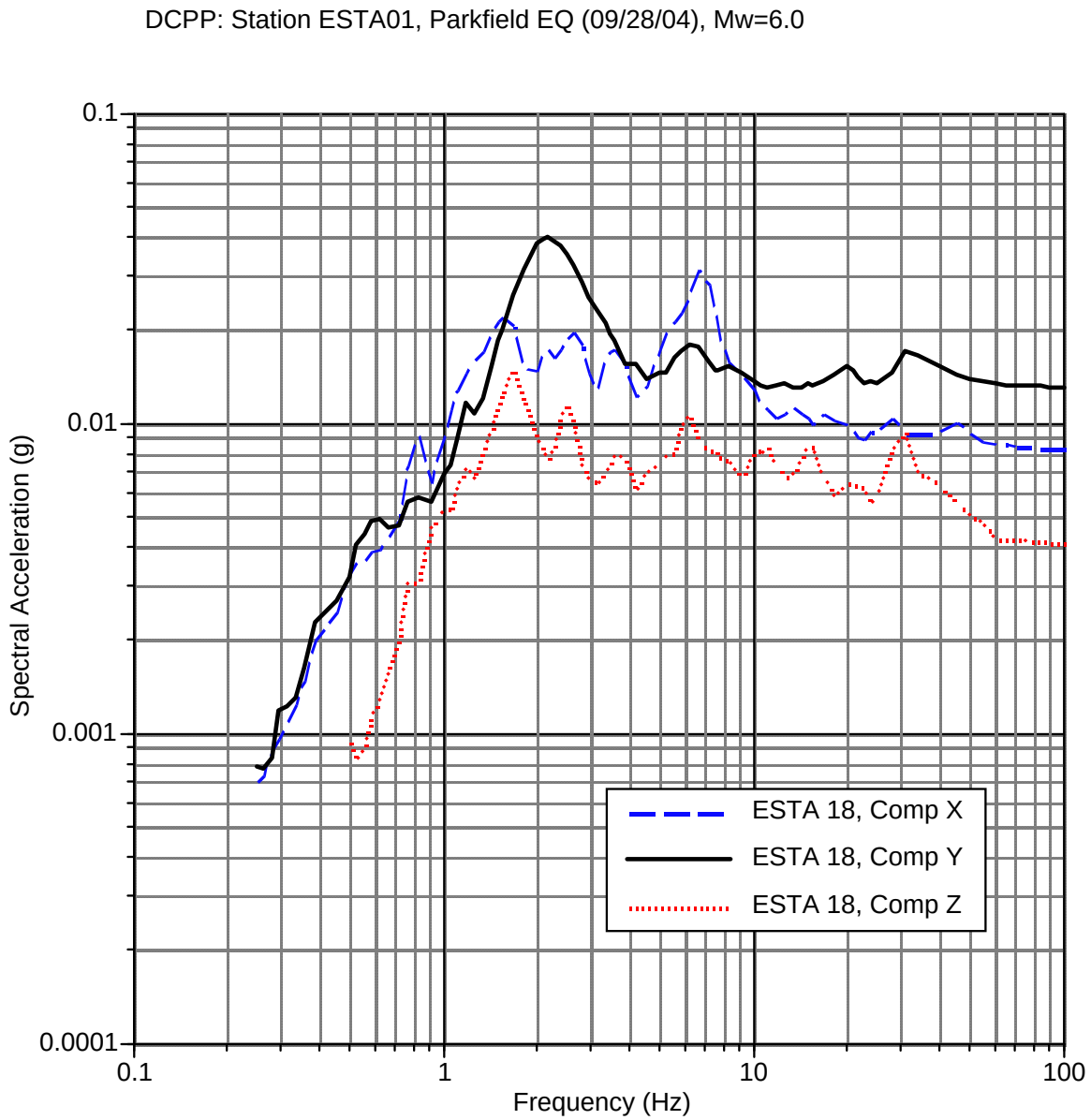

Figure 25. Response spectra at 5% damping for ESTA 18 (100' elev U1 Aux Building).

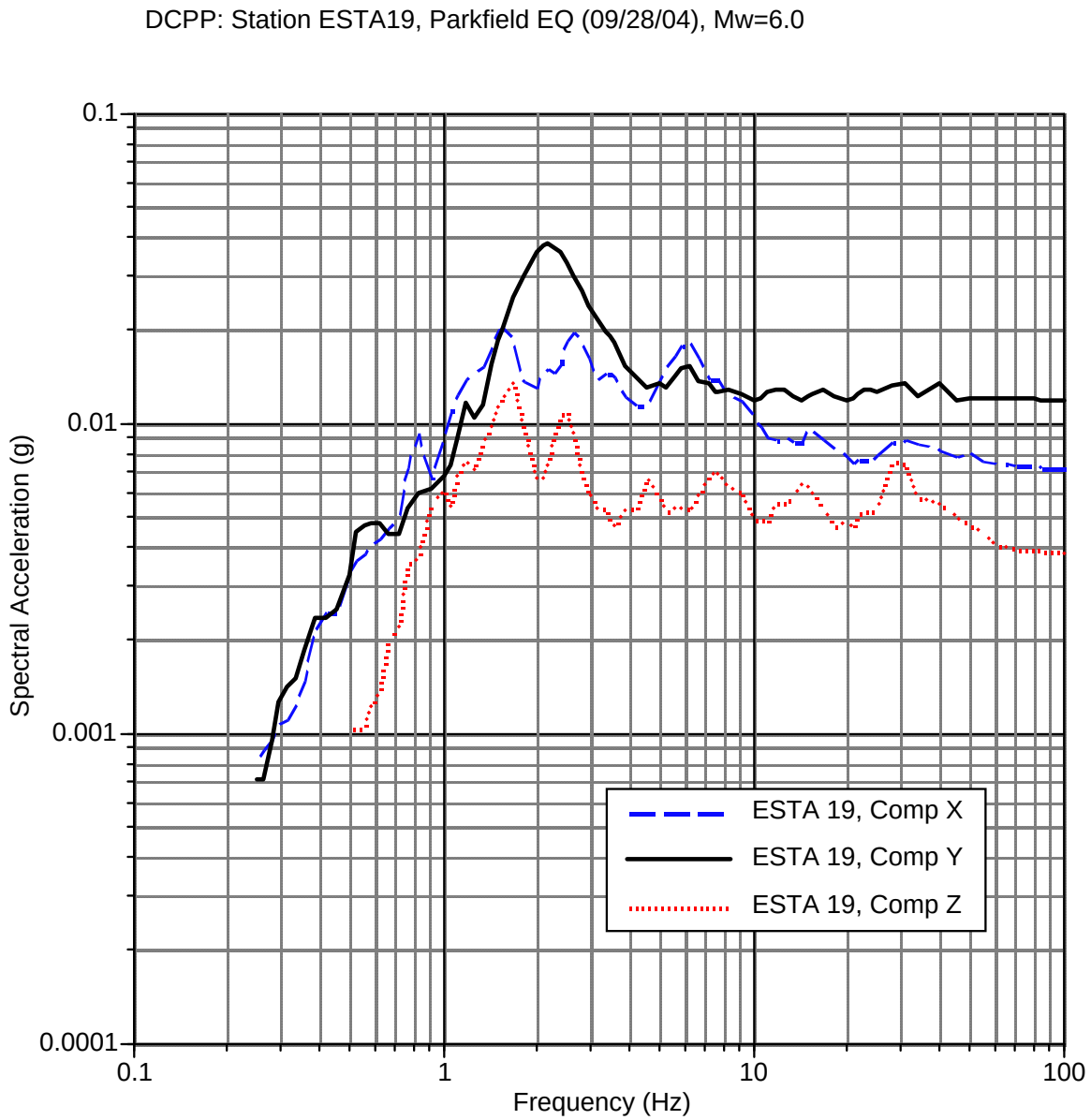

Figure 26. Response spectra at 5% damping for ESTA 19 (100' elev U1 & U2 Aux Building).

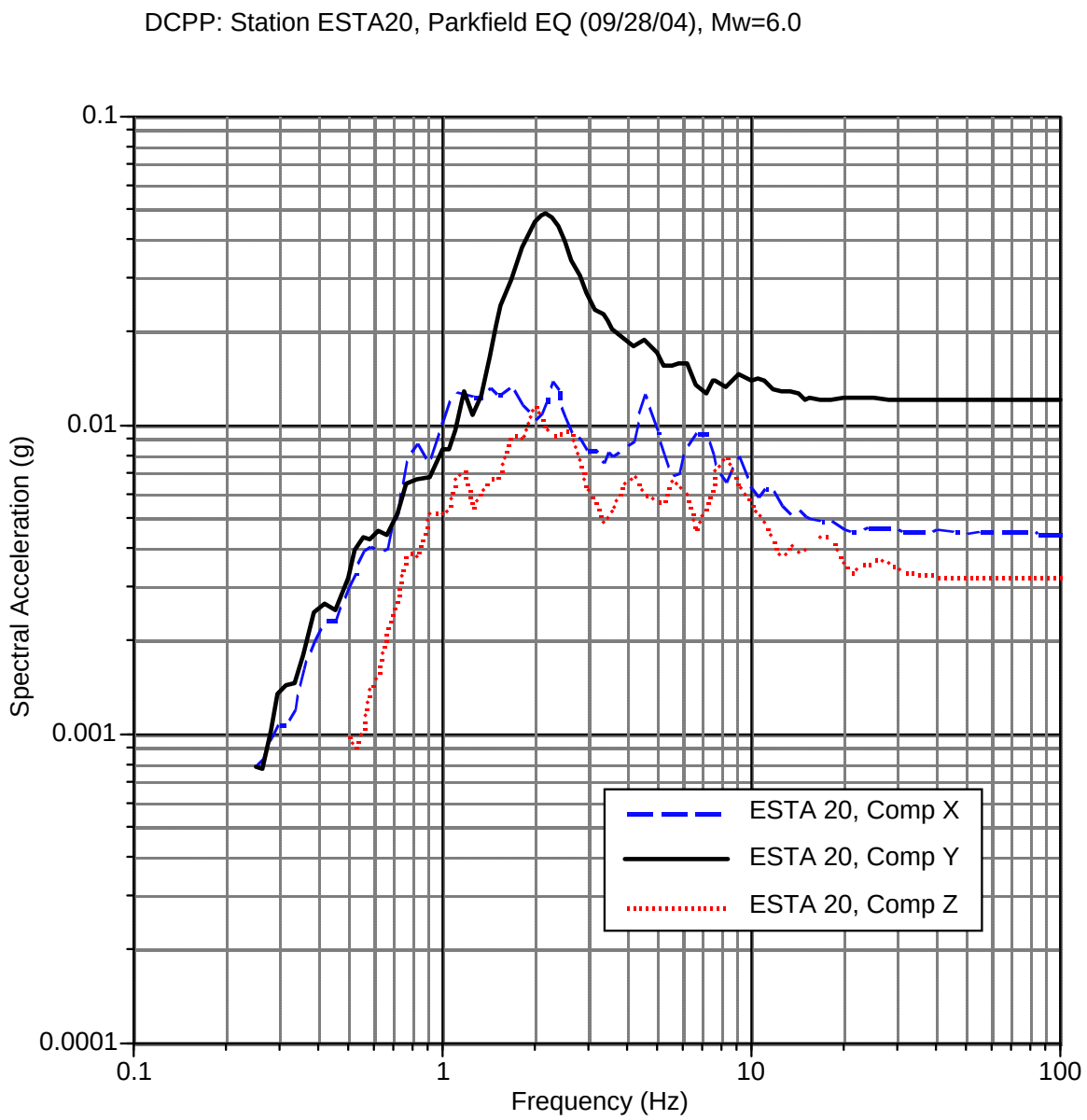

Figure 27. Response spectra at 5% damping for ESTA 20 (Free Field near Raw Water reservoirs).

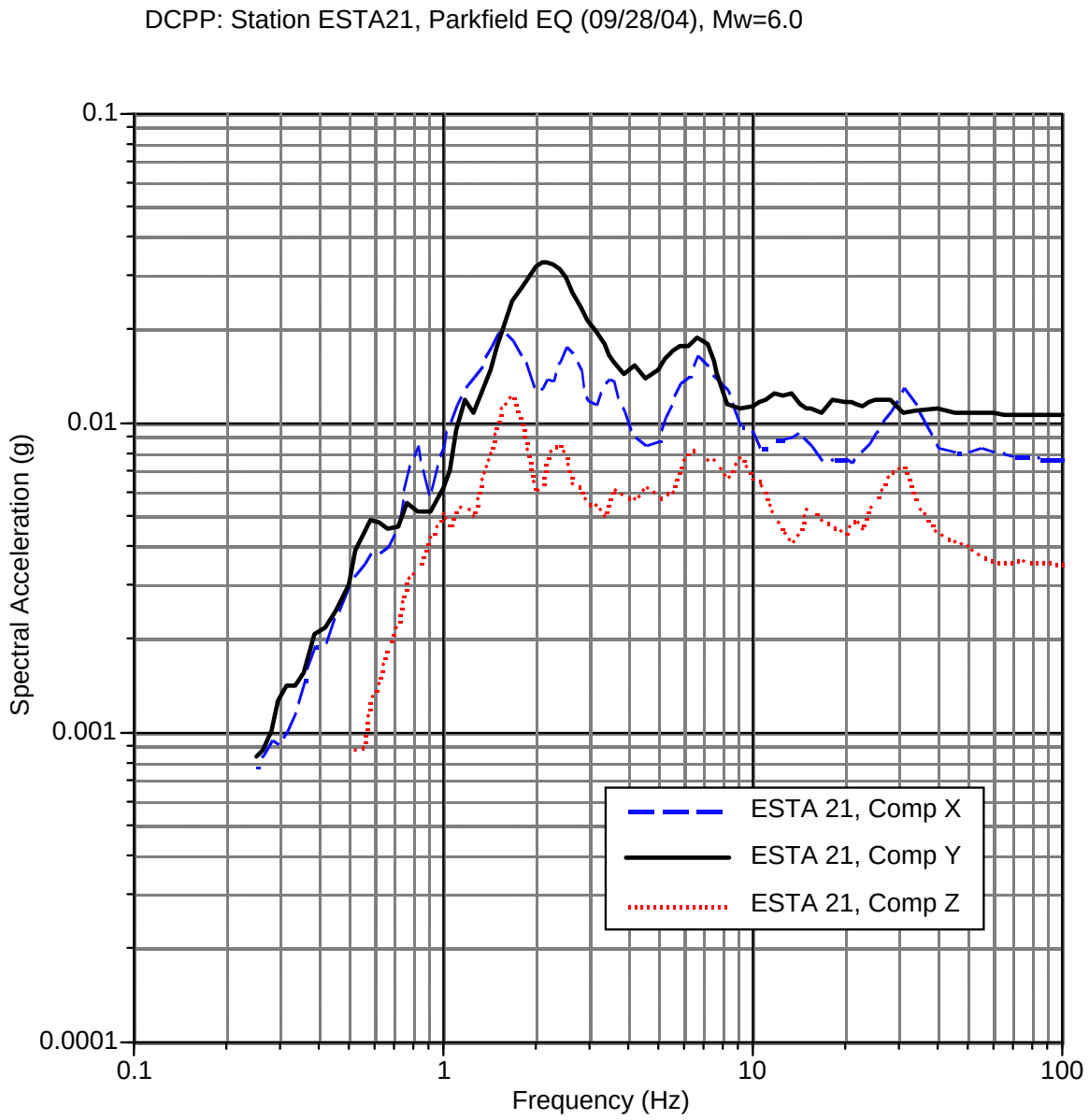

Figure 28. Response spectra at 5% damping for ESTA 21 (85' elev. U1 Turb Bldg North end of switch gear room).

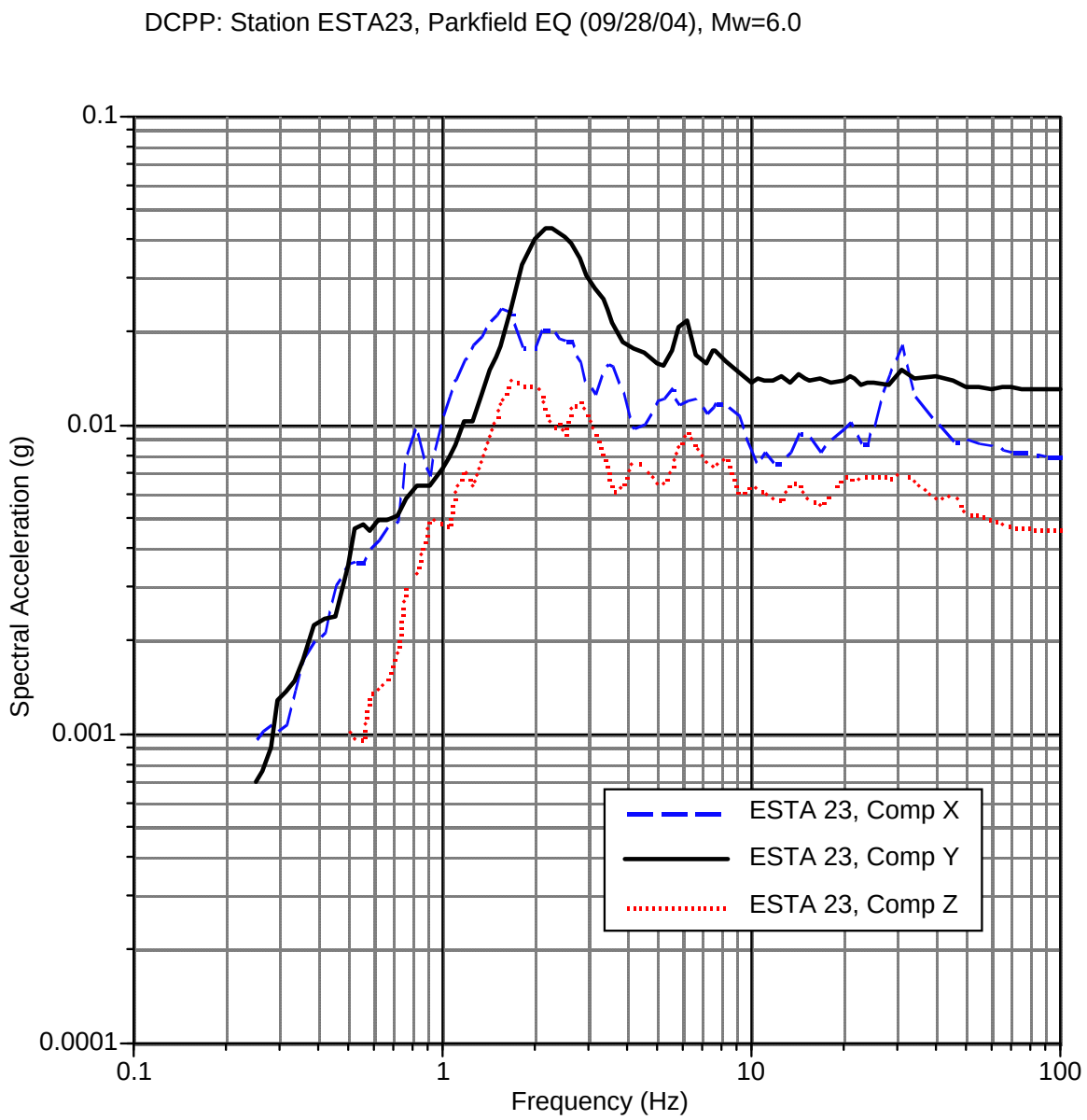

Figure 29. Response spectra at 5% damping for ESTA 23 (85' elev. U2 Turbine Building South end Stairs).

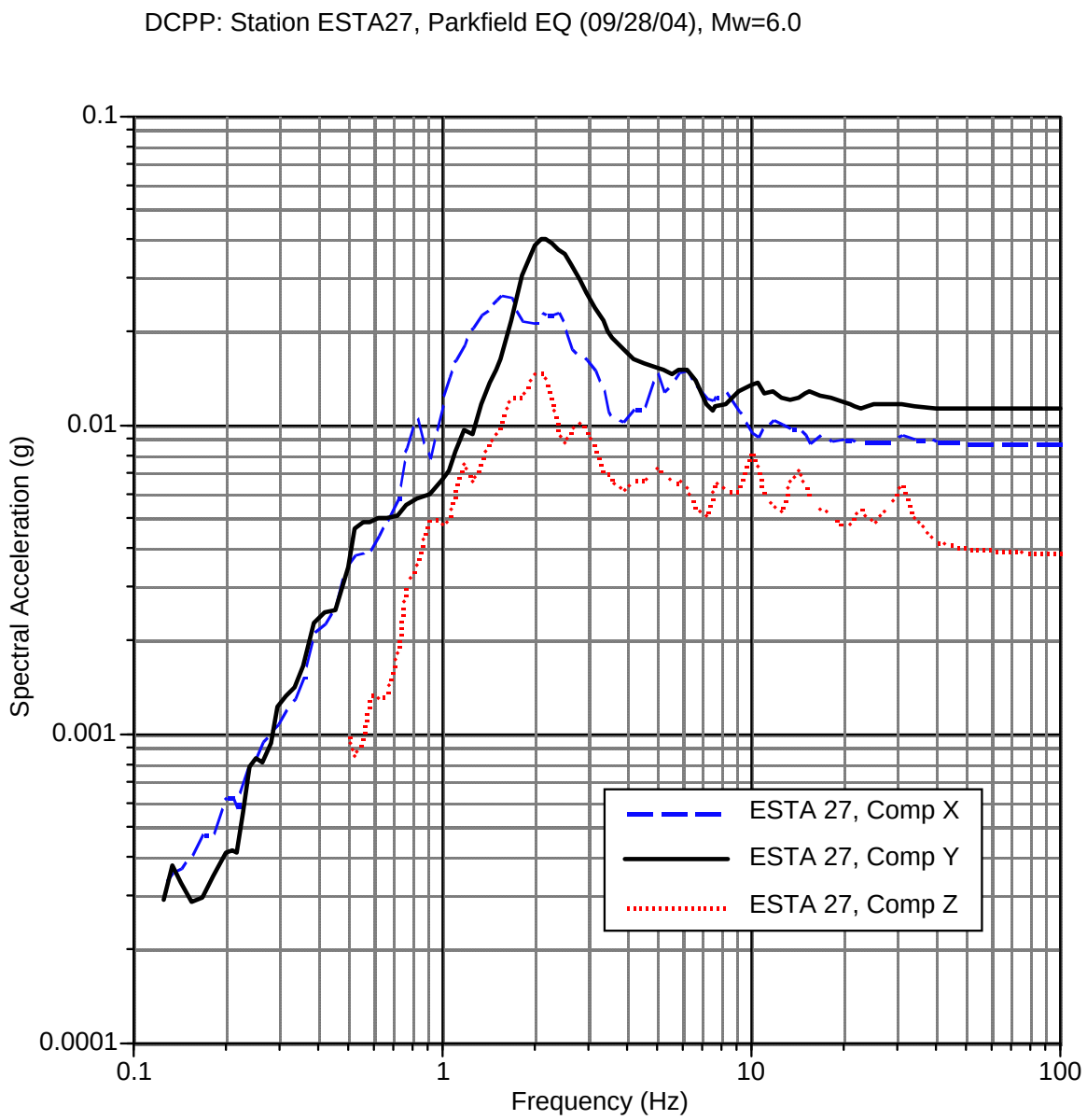

Figure 30. Response spectra at 5% damping for ESTA 27 (82' elev. Free Field in underground vault near Fitness Trailer).

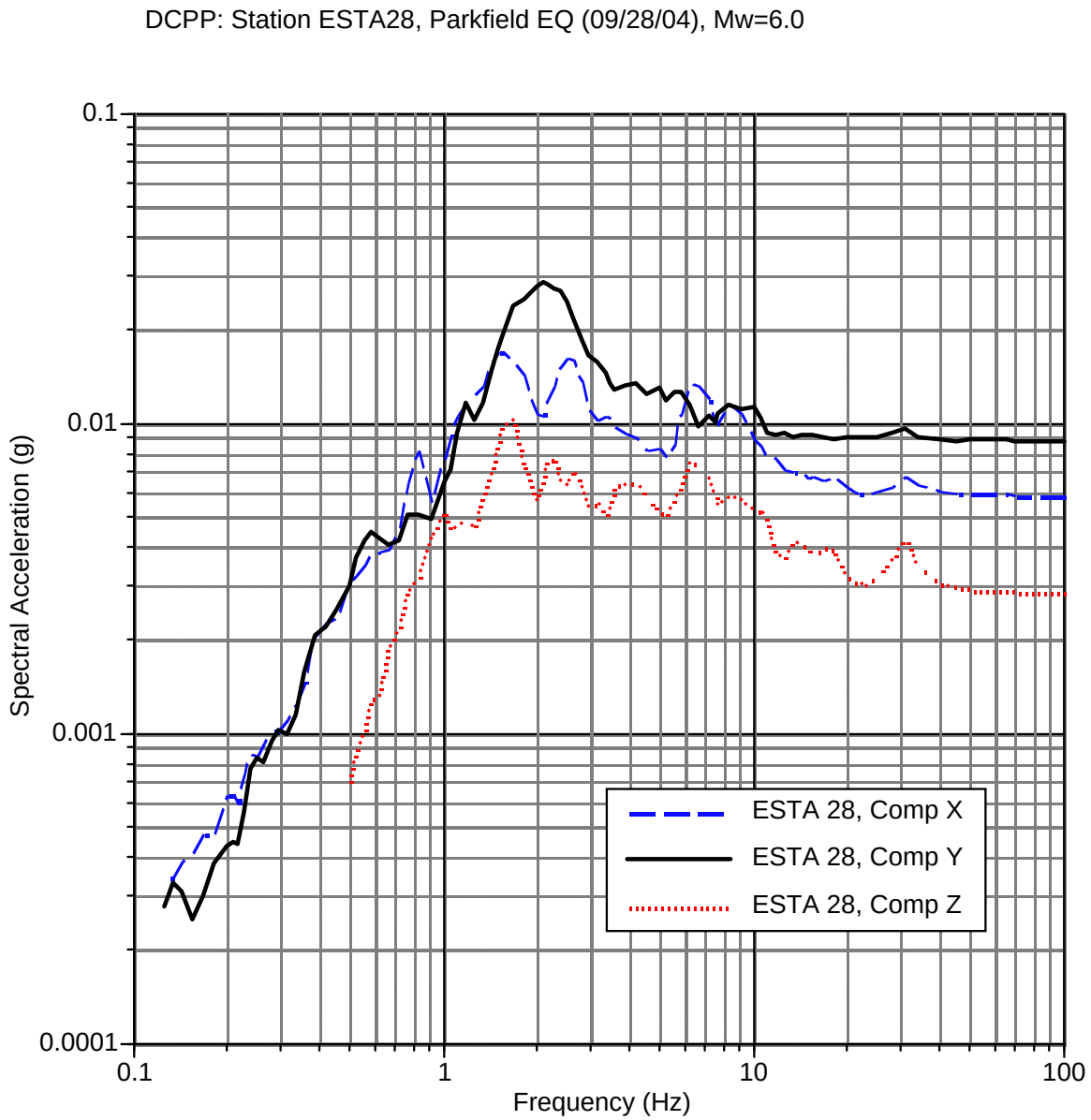

Figure 31. Response spectra at 5% damping for ESTA 28 (85' elev. Free Field in paved area north of U1 containment).

Table 1. Peak values from the DCPP recordings of the 2004 Parkfield Earthquake after filtering and baseline corrections. See Figures 6 and 7 for instrument locations.

	PGA(g)			PGV (cm/s)			PGD (cm)		
Station	X	Y	Z	X	Y	Z	X	Y	Z
ESTA01	0.0069	0.0119	0.0045	0.711	0.990	0.310	0.127	0.128	0.044
ESTA02	0.0137	0.0220	0.0080	0.985	1.329	0.366	0.169	0.183	0.068
ESTA03	0.0065	0.0105	0.0032	0.682	0.907	0.317	0.124	0.112	0.043
ESTA04	0.0075	0.0121	0.0046	0.717	0.958	0.324	0.131	0.120	0.042
ESTA05	0.0072	0.0115	0.0036	0.651	0.883	0.310	0.119	0.100	0.043
ESTA08	0.0118	0.0118	0.0051	0.0727	1.012	0.324	0.125	0.130	0.044
ESTA09	0.0105	0.0124	0.0051	0.799	1.071	0.331	0.124	0.119	0.046
ESTA10	0.0087	0.0127	0.0050	0.752	0.964	0.358	0.136	0.123	0.047
ESTA14	0.0077	0.0133	0.0051	0.696	1.036	0.367	0.127	0.125	0.042
ESTA15	0.0075	0.0128	0.0044	0.671	1.017	0.297	0.116	0.122	0.049
ESTA16	0.0075	0.0128	0.0041	0.735	0.906	0.352	0.129	0.104	0.042
ESTA17	0.0074	0.0113	0.0032	0.687	0.912	0.323	0.111	0.043	0.179
ESTA18	0.0083	0.0131	0.0041	0.741	0.971	0.299	0.122	0.119	0.041
ESTA19	0.0072	0.0119	0.0038	0.691	0.965	0.328	0.129	0.132	0.044
ESTA20	0.0045	0.0120	0.0032	0.0628	0.965	0.293	0.113	0.125	0.044
ESTA21	0.0077	0.0106	0.0035	0.733	0.903	0.309	0.117	0.113	0.038
ESTA23	0.0079	0.0131	0.0046	0.738	1.007	0.284	0.139	0.128	0.039
ESTA27	0.0087	0.0113	0.0039	0.882	0.966	0.289	0.163	0.154	0.040
ESTA28	0.0059	0.0088	0.0028	0.684	0.774	0.295	0.179	0.152	0.037